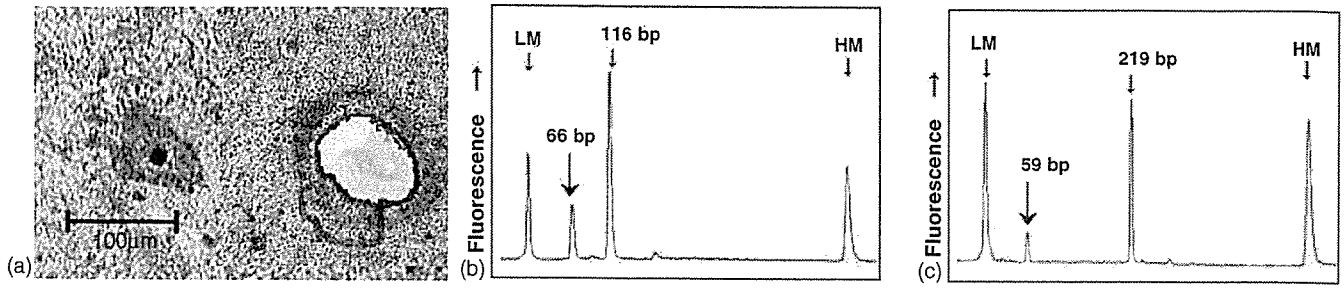

Fig. 1. (a) A single motor neuron from an SBMA patient before (left) and after (right) the dissection with a laser-microdissector. (b and c) An example of electropherogram by a 2100 Bioanalyser. Samples are the Bbv-1-digest of PCR product from tissues of a single motor neuron from an SBMA patient (b) and from a mutated human $SOD1^{G93A}$ transgenic mouse (c). LM: lower marker (15 bp), HM: higher marker (600 bp).

neurons of mutated human SOD1 transgenic rats yielded only 219 and 59 bp fragments (Fig. 1). Therefore, the values of RNA editing efficiency at the Q/R site of GluR2 were 100% in 44 motor neurons from three SBMA cases (Table 1), 55 single motor neurons from three $SOD1^{G93A}$ transgenic rats, 62 neurons from three $SOD1^{H46R}$ transgenic rats, as well as in 42 neurons from three littermate rats of each group (Table 2). The consistent finding that the GluR2 Q/R site is 100% edited in motor neurons of SBMA patients and transgenic rats for mutated human SOD1 is in marked contrast to the finding in ALS motor neurons that the editing efficiency widely varied among neurons ranging from 0% to 100% (Kawahara et al., 2004).

4. Discussion

Compared to the significant underediting reported for the GluR2 Q/R site in motor neurons of sporadic ALS (Kawahara et al., 2004), GluR2 mRNA in all the examined motor neurons of the mutated human SOD1 transgenic rats with two different mutation sites and SBMA patients was completely edited at the Q/R site. We have confirmed that postmortem delay hardly influenced the editing efficiency at the GluR2 Q/R site (Kawahara et al., 2003b), hence the significant difference in the postmortem delay between the SBMA patients in this study and ALS patients in the previous report (Kawahara et al., 2004) would not have affected these results. We examined the motor neurons in the spinal cord segment corresponding to the hindlimb of mutated human SOD1 transgenic rats after their hindlimbs had become weak, indicating that the motor neurons examined were already pathologically affected. Likewise, we found that only a small number of motor neurons remained in the spinal cord of SBMA patients. Thus our results indicate that GluR2 RNA editing was complete in the dying motor neurons in both the mutated human SOD1 transgenic rats and SBMA patients, implying that the neuronal death mechanism is not due to the underediting of GluR2 mRNA seen in sporadic ALS. Since the pathogenic mechanism underlying ALS1 is considered to be the same as in mutant human SOD1 transgenic animals, motor neurons in affected ALS1 patients would be expected to have only edited GluR2 mRNA. Indeed, an association study of the SOD1 gene in a considerable number of patients with sporadic ALS reported no significant association with mutations of the SOD1 gene (Jackson et al., 1997). Due to the lack of appropriate animal model for sporadic ALS, mutant human SOD1 transgenic animals have been used as a model for ALS in general, particularly in studies searching for therapeutically effective drugs. However, it should be kept in mind that mutated human SOD1 transgenic animals are merely a suggestive model for sporadic ALS and a gain of toxic function in mutated SOD1 kills motor neurons via mechanisms other than the demise of RNA editing. There are likely multiple different death pathways in motor neurons, and motor neurons in sporadic ALS, ALS1 and SBMA die by different death cascades.

Acknowledgements

This investigation was supported in part by grants-in-aid for Scientific Research on Priority Areas from the Ministry of Education, Culture, Sports, Science and Technology of Japan and grants from the Ministry of Health, Labor and Welfare of Japan (to SK), and a grant from Japan ALS Association (to YK).

References

Brusa, R., Zimmermann, F., Koh, D., Feldmeyer, D., Gass, P., Seeburg, P., Sprengel, R., 1995. Early-onset epilepsy and postnatal lethality associated with an editing-deficient GluR-B allele in mice. Science 270, 1677–1680.

Burnashev, N., Monyer, H., Seeburg, P., Sakmann, B., 1992. Divalent ion permeability of AMPA receptor channels is dominated by the edited form of a single subunit. Neuron 8, 189–198.

Hume, R.I., Dingledine, R., Heinemann, S.F., 1991. Identification of a site in glutamate receptor subunits that controls calcium permeability. Science 253, 1028–1031.

Jackson, M., Al-Chalabi, A., Enayat, Z.E., Chioza, B., Leigh, P.N., Morrison, K.E., 1997. Copper/zinc superoxide dismutase 1 and sporadic amyotrophic lateral sclerosis: analysis of 155 cases and identification of a novel insertion mutation. Ann. Neurol. 42, 803–807.

Katsuno, M., Adachi, H., Doyu, M., Minamiyama, M., Sang, C., Kobayashi, Y., Inukai, A., Sobue, G., 2003. Leuprorelin rescues polyglutamine-dependent phenotypes in a transgenic mouse model of spinal and bulbar muscular atrophy. Nat. Med. 9, 768–773.

Katsuno, M., Adachi, H., Kume, A., Li, M., Nakagomi, Y., Niwa, H., Sang, C., Kobayashi, Y., Doyu, M., Sobue, G., 2002. Testosterone reduction prevents phenotypic expression in a transgenic mouse model of spinal and bulbar muscular atrophy. Neuron 35, 843–854.

Kawahara, Y., Ito, K., Sun, H., Aizawa, H., Kanazawa, I., Kwak, S., 2004. RNA editing and death of motor neurons. Nature 427, 801.

Kawahara, Y., Ito, K., Sun, H., Kanazawa, I., Kwak, S., 2003a. Low editing efficiency of GluR2 mRNA is associated with a low relative abundance of

ADAR2 mRNA in white matter of normal human brain. Eur. J. Neurosci. 18, 23–33.

Kawahara, Y., Kwak, S., Sun, H., Ito, K., Hashida, H., Aizawa, H., Jeong, S.-Y., Kanazawa, I., 2003b. Human spinal motoneurons express low relative abundance of GluR2 mRNA: an implication for excitotoxicity in ALS. J. Neurochem. 85, 680–689.

Kuner, R., Groom, A.J., Bresink, I., Kornau, H.C., Stefovska, V., Muller, G., Hartmann, B., Tschauner, K., Waibel, S., Ludolph, A.C., Ikonomidou, C., Seeburg, P.H., Turski, L., 2005. Late-onset motoneuron disease caused by a functionally modified AMPA receptor subunit. Proc. Natl. Acad. Sci. U.S.A. 102, 5826–5831.

Kwak, S., Kawahara, Y., 2005. Deficient RNA editing of GluR2 and neuronal death in amyotropic lateral sclerosis. J. Mol. Med. 83, 110–120.

La Spada, A.R., Wilson, E.M., Lubahn, D.B., Harding, A.E., Fischbeck, K.H., 1991. Androgen receptor gene mutations in X-linked spinal and bulbar muscular atrophy. Nature 352, 77–79.

Nagai, M., Aoki, M., Miyoshi, I., Kato, M., Pasinelli, P., Kasai, N., Brown Jr., R.H., Itoyama, Y., 2001. Rats expressing human cytosolic copper–zinc superoxide dismutase transgenes with amyotrophic lateral sclerosis: associated mutations develop motor neuron disease. J. Neurosci. 21, 9246–9254.

Rosen, D.R., Siddique, T., Patterson, D., Figlewicz, D.A., Sapp, P., Hentati, A., Donaldson, D., Goto, J., O'Regan, J.P., Deng, H.X., et al., 1993. Mutations in Cu/Zn superoxide dismutase gene are associated with familial amyotrophic lateral sclerosis. Nature 362, 59–62.

Takuma, H., Kwak, S., Yoshizawa, T., Kanazawa, I., 1999. Reduction of GluR2 RNA editing, a molecular change that increases calcium influx through AMPA receptors, selective in the spinal ventral gray of patients with amyotrophic lateral sclerosis. Ann. Neurol. 46, 806–815.

Verdoorn, T., Burnashev, N., Monye, R.H., Seeburg, P., Sakmann, B., 1991. Structural determinants of ion flow through recombinant glutamate receptor channels. Science 252, 1715–1718.

Journal of Neurochemistry, 2006, **98**, 782–791 doi:10.1111/j.1471-4159.2006.03903.x

Slow and selective death of spinal motor neurons *in vivo* by intrathecal infusion of kainic acid: implications for AMPA receptor-mediated excitotoxicity in ALS

Hui Sun,*[,1] Yukio Kawahara,*[,2] Kyoko Ito,* Ichiro Kanazawa† and Shin Kwak*

**Department of Neurology, Graduate School of Medicine, The University of Tokyo, Tokyo, Japan*

†National Center of Neurology and Psychiatry, SORST Japan Science and Technology Corporation, Tokyo, Japan

Abstract

Excitotoxicity mediated by α-amino-3-hydroxy-5-methyl-4-isoxazole propionic acid (AMPA) receptors has been proposed to play a major role in the selective death of motor neurons in sporadic amyotrophic lateral sclerosis (ALS), and motor neurons are more vulnerable to AMPA receptor-mediated excitotoxicity than are other neuronal subclasses. On the basis of the above evidence, we aimed to develop a rat model of ALS by the long-term activation of AMPA receptors through continuous infusion of kainic acid (KA), an AMPA receptor agonist, into the spinal subarachnoid space. These rats displayed a progressive motor-selective behavioral deficit with delayed loss of spinal motor neurons, mimicking the clinicopathological characteristics of ALS. These changes were significantly ameliorated by co-infusion with 6-nitro-7-sulfamobenso(f)quinoxaline-2,3-dione (NBQX), but not with D(–)-2-amino-5-phosphonovaleric acid (APV), and were exacerbated by co-infusion with cyclothiazide, indicative of an AMPA receptor-mediated mechanism. Among the four AMPA receptor subunits, expression of GluR3 mRNA was selectively up-regulated in motor neurons but not in dorsal horn neurons of the KA-infused rats. The up-regulation of GluR3 mRNA in this model may cause a molecular change that induces the selective vulnerability of motor neurons to KA by increasing the proportion of GluR2-lacking (i.e. calcium-permeable) AMPA receptors. This rat model may be useful in investigating ALS etiology.

Keywords: amyotrophic lateral sclerosis, AMPA receptor, excitotoxicity, GluR3, GluR2, RNA editing.

J. Neurochem. (2006) **98**, 782–791.

The most common motor neuron disease, amyotrophic lateral sclerosis (ALS), is a progressive neurodegenerative disease characterized by selective upper and lower motor neuron loss that is initiated in mid-life and leads to death as a result of respiratory muscular weakness. ALS has a uniform worldwide prevalence (five cases per 100 000 individuals), of which sporadic ALS accounts for more than 90% of all cases and only the remaining 5% of cases are familial (FALS) (Roland *et al.* 2005). Despite the fact that a good animal model is indispensable for investigating the etiology and for developing novel therapies for a disease, few appropriate animal models for sporadic ALS have been developed. Among the animal models tested, animal lines transgenic for the mutated human *Cu/Zn superoxide dismutase* (*SOD1*) gene (Gurney *et al.* 1994; Nagai *et al.* 2001; Howland *et al.* 2002) are regarded as a candidate disease model for all types of ALS, but the etiology of the FALS caused by the *SOD1* gene mutation is not necessarily the same as that of sporadic ALS. Indeed, the extent of neuropathological changes is not confined to motor neurons in these animals (Gurney *et al.* 1994), and although *SOD1* gene mutations have been found in a small population of patients with sporadic ALS, no significant association has been detected between sequence variants in the SOD1 locus and sporadic ALS

Received January 6, 2006; revised manuscript received March 15, 2006; accepted March 20, 2006.

Address correspondence and reprint requests to Shin Kwak MD PhD, Department of Neurology, Graduate School of Medicine, The University of Tokyo, 7-3-1 Hongo, Bunkyo-ku, Tokyo 113–8655, Japan.
E-mail: kwak-tky@umin.ac.jp

[1]Present address: National Institute for Longevity Sciences, Obu, Japan.
[2]Present address: the Wistar Institute, Philadelphia, PA, USA.

Abbreviations used: aCSF, artificial cerebrospinal fluid; ALS, amyotrophic lateral sclerosis; AMPA, α-amino-3-hydroxy-5-methyl-4-isoxazole propionic acid; APV, D(–)-2-amino-5-phosphonovaleric acid; CTZ, cyclothiazide; F, Fischer; FALS, familial ALS; KA, kainic acid; NBQX, 6-nitro-7-sulfamobenso(f)quinoxaline-2,3-dione; PBS, phosphate-buffered saline; SOD1, Cu/Zn superoxide dismutase; W, Wistar.

21

susceptibility or phenotype (Jackson *et al.* 1997; Broom *et al.* 2004). Furthermore, the underediting of GluR2 mRNA at the Q/R site, which is a specific molecular change in sporadic ALS motor neurons (Kawahara *et al.* 2004), does not occur in degenerating motor neurons in rats transgenic for mutated human *SOD1* (Kawahara *et al.* 2006). Although *SOD1* transgenic animals have been used widely, these cannot be used as a model for sporadic ALS. On the other hand, a mouse line transgenic for Ca^{2+}-permeable artificial GluR-B(N) has been reported to develop motor neuron loss after 12 months of survival (Feldmeyer *et al.* 1999; Kuner *et al.* 2005), and therefore may be similar to sporadic ALS with respect to etiology, but this model has not been widely used.

Motor neurons in the spinal cord are differentially more vulnerable to α-amino-3-hydroxy-5-methyl-4-isoxazole propionic acid (AMPA) receptor-mediated excitotoxicity than are other neuronal subsets *in vitro* owing to an increased flux of Ca^{2+} through AMPA receptor channels (Carriedo *et al.* 1996). Ca^{2+} influx through AMPA receptors is regulated by either the presence or the absence of a GluR2 subunit: AMPA receptors containing GluR2 have a low Ca^{2+} influx, whereas those containing no GluR2 have a high Ca^{2+} influx (Hollmann *et al.* 1991; Verdoorn *et al.* 1991; Burnashev *et al.* 1992). However, when AMPA receptors contain a GluR2 subunit translated from unedited mRNA, their Ca^{2+} permeability remains high (Sommer *et al.* 1991). Therefore, both deficiency in GluR2 expression and underediting of GluR2 mRNA can induce AMPA receptor-mediated neuronal death. It is therefore interesting to investigate whether the AMPA receptor-mediated slow death of motor neurons occurs *in vivo* and what molecular changes occur in the AMPA receptor subunits. Here we induced the selective death of motor neurons in adult rats by a continuous infusion of kainic acid (KA) into the spinal subarachnoid space. Because slowly progressive and selective neuronal death is a hallmark of degenerative neurological diseases, such a model is useful to investigate the mechanism underlying the selective death of motor neurons in ALS.

Materials and methods

Operation

Each test compound was dissolved in artificial cerebrospinal fluid (aCSF; 122 mM NaCl, 3.1 mM KCl, 5 mM $NaHCO_3$, 0.4 mM KH_2PO_4, 1.3 mM $CaCl_2$, 1.0 mM $MgSO_4$ and 10 mM D-glucose, pH 7.4) with the pH adjusted to 7.2, and the resulting solution was used to fill an Alzet Model 2004 osmotic minipump (capacity 200 μL, pump speed 0.25 μL/ h; DURECT Corp., Cupertino CA, USA), which was incubated in sterile saline solution at 37°C overnight before operation after connection with a PE10 cannula (inner diamater, 0.25 mm; outer diamater, 0.55 mm; EICOM Corp., Tokyo, Japan). The operation was performed with slight modifications to the protocol described by Nakamura *et al.* (1994, 1997). In brief, male Wistar (W; body weight 180–250 g) and Fischer (F; body weight 110–160 g) rats (Japanese Oriental Yeast Co. Ltd, Shizuoko, Japan) were laminectomized at L5/6 under deep pentobarbiturate anesthesia, the free end of the PE10 cannula was inserted into the lumber spinal subarachnoid space, and the osmotic minipump was placed subcutaneously in the back.

Either W or F rats were infused with 3 mM KA (Sigma-Aldrich Corp., St Louis, MO, USA) continuously for 2 (KA-W2, KA-F2), 4 (KA-W4, KA-F4) or 8 (KA-W8) weeks. As controls, either W (aCSF-W) or F (aCSF-F) rats were infused with aCSF in the same manner for the same period of KA infusion (i.e. 2, 4 or 8 weeks). In some experiments, in order to investigate the neurotoxic mechanism, male F rats were infused intrathecally for either 2 or 4 weeks with one of the following combinations of glutamate receptor-acting drugs: 3 mM KA plus 3 mM 6-nitro-7-sulfamoyl-benzo(f)quinoxaline-2,3-dione (NBQX; TOCRIS Cookson Ltd, Bristol, UK) (KA/NBQX group); 3 mM KA plus 3 mM D(−)-2-amino-5-phosphonopentanoic acid (APV; TOCRIS NEURAMIN, Buckhurst Hill, Essex, UK) (KA/APV group); 1.5 mM cyclothiazide (CTZ; TOCRIS, Ellisville, MO, USA) (CTZ group); or 1.5 mM KA plus 1.5 mM CTZ (KA/CTZ group). In the KA/CTZ and CTZ groups, the osmotic minipump was replaced every week with one refilled with freshly prepared 1.5 mM KA plus 1.5 mM CTZ solution and 1.5 mM CTZ solution, respectively.

Animals were handled according to the protocols approved by the Institutional Animal Care and Use Committee in line with the *Guide for the Care and Use of Laboratory Animals* of the National Institutes of Health.

Evaluation of movement behavior

Throughout the experimental period, the movement behavior of rats was measured each week, mainly by using a rat-specific rotarod (SN-445; Neuroscience Corp., Tokyo Japan), which constantly rotated at a speed of 16 rpm and automatically recorded the time that rats could stay on the rotarod during a 420-second period. The rotarod scores of rats were recorded on average in three separate trials. Paralysis was scored when the rat dragged one of its hindlimbs. Rats were also tested for whether they exhibited an escape response from the pain elicited by stimulation of the hindlimbs with tweezers, and whether they had urinary and/or fecal incontinence.

Spinal cord samples

The rats were anesthetized deeply using diethyl ether inhalant, after which their spinal cords were quickly removed and frozen in liquid nitrogen. The samples were stored at −80°C until use. The frozen spinal cord samples were obtained from KA-W2, KA-W4 and KA-W8 (n = 5 each); KA-F2 and KA-F4 (n = 5 each); KA/NBQX (n = 5); KA/APV (n = 5); KA/CTZ (n = 5); CTZ (n = 5); aCSF-W2, aCSF-W4 and aCSF-W8 (n = 5 each); and aCSF-F2 and aCSF-F4 (n = 5 each) rats.

For morphological analysis, rats were perfused transcardially with 3.5% paraformaldehyde and 0.5% glutaraldehyde in 0.1 M phosphate-buffered saline (PBS; pH 7.6). The spinal cords of KA-W4 and KA-W8 (n = 3 each), KA-F2 and KA-F4 (n = 3 each), KA-NBQX (n = 3), KA/CTZ at 2 and 4 weeks (n = 5 each), CTZ (n = 5), aCSF-W4 and aCSF-W8 (n = 3 each), and aCSF-F2

and aCSF-F4 ($n = 5$ each) rats were removed and postfixed in the same fixative at 4°C for 12 h.

Neuropathology

The lumber segments of spinal cords fixed in paraformaldehyde and glutaraldehyde were dehydrated overnight at 4°C with serial concentrations of sucrose (5%, 10%, 15%, 20%, 25% and 30%), and then rapidly frozen on dry ice. Thirty serial 20-μm-thick frozen sections were made with a cryostat (Model HM500 O; MICROM, Walldorf, Germany) and stained with either 0.1% Cresyl violet (pH 3.5) or hematoxylin and eosin. The number of neurons the diameters of which were greater than 20 μm and had identifiable nucleoli was counted in the ventral horns of the spinal cord under a light microscope, and their morphology was also observed.

To determine the morphological changes in the axons of motor neurons, L5 ventral roots of KA-W8 ($n = 3$), KA/CTZ ($n = 3$) and their respective control rats ($n = 3$ each) were postfixed with 2.0% paraformaldehyde and 2.0% glutaraldehyde in 0.1 M PBS, and mounted in resin. Transverse 1-μm-thick Epon-embedded sections of L5 ventral roots were made and stained with 0.1% toluidine blue and viewed under a light microscope.

Single-cell dissection

Single-cell isolation was carried out using an excimer laser microdissection system (Hamamatua Photonics Ltd, Shizuoka, Japan) as previously described (Hashida *et al.* 2001; Kawahara *et al.* 2003; Sun *et al.* 2005). In brief, 20-μm-thick frozen sections were attached to glass slides made of artificial quartz, fixed with 100% methanol for 60 s and then stained with 0.1% toluidine blue. Thirty spinal motor neurons (Motor) were dissected free and placed in test-tubes containing 200 μL of TRIZOL reagent (Invitrogen Corp., Carlsbad, CA, USA). The substantia gelatinosa, ventral and dorsal funiculi of the spinal cord were dissected *en bloc* and placed in tubes containing 200 μL of TRIZOL reagent in a similar manner. All samples were stored at −20°C until use.

RNA extraction and reverse transcription

Total RNA was extracted from each tissue sample using TRIZOL reagent according to the manufacturer's instructions. Single-cell RNA extraction and reverse transcription procedures were carried out as previously described (Hashida *et al.* 2001; Kawahara *et al.* 2003; Sun *et al.* 2005). Reverse transcription was performed with either Ready-to-go You-Prime First-Strand beads (Amersham Biosciences Corp., Piscataway, NJ, USA) or 0.5 μM oligo(dT) primer for tissue samples, or with a Sensiscript RT Kit (QIAGEN GmbH, Hilden, Germany) using 0.5 mM oligo(dT) primer and 10 U of prime RNase inhibitor (Eppendorf AG, Hamburg, Germany) for the single-cell samples. The cDNAs were stored at −20°C until use.

Real-time quantitative PCR

The primer sets for the internal standard of GluR1–R4 and β-actin have been described elsewhere (Sun *et al.* 2005). Each PCR reaction was run in 50 μL of the reaction mixture containing each primer at 200 μM, 1 mM dNTP MIX, 5 μL of 10 × PCR buffer and 1 μL of Ampli Taq DNA polymerase (Applied Biosystems, Roche Molecular Systems Inc., Branchburg, NJ, USA). The PCR amplification conditions were 95°C for 2 min, followed by 35 cycles of 95°C for 30 s, 60°C for 30 s and 72°C for 1 min. The PCR products were then purified with a Zymoclean Gel DNA Recovery Kit (Zymo Research, Orange, CA, USA). The concentration of PCR products was determined with a spectrophotometer (Nano Drop™ ND-1000; Nano Drop Technologies Inc., Wilmington, DE, USA). We prepared serial dilutions with 10^8–10^6, 10^6–10^4, 10^4–10^3, 10^3–10^2 and 10^3–10^1 copies per 2 μL, which contained 100 ng of herring sperm DNA in Tris-EDTA buffer (pH 8.0).

The procedure was performed as described previously (Kawahara *et al.* 2003; Sun *et al.* 2005). In brief, quantitative PCR was performed with a LightCycler System (Roche Diagnostics, Mannheim, Germany). The PCR primers and probes for GluR1, GluR4 and β-actin comprised approximately 180–250 base pairs and matched sequences in the 3′ untranslated regions (UTR) in order to avoid the flip/flop and GluR4c alternative splicing sites. Moreover, phosphate groups were attached to the 3′ end of the LCRed640-containing probes to prevent probe extension. A set of standards and cDNA samples was amplified in duplicate in a reaction mixture (20 μL of total volume) containing 2 μL of 10 × FastStart Taq DNA polymerase, 4 mM $MgCl_2$, each primer at 0.5 mM, 0.2 μM fluorescein isothiocyanate (FITC)-containing probe and 0.4 μM LCRed640-containing probe. Herring sperm DNA solution was included as a negative control in each series of reactions. The reactions were initiated by the activation of FastStart Taq DNA polymerase at 95°C for 10 min, and amplification was achieved by running 45 cycles of denaturation at 95°C for 1 s, annealing at 58°C for 10 s, and extension at 72°C for 12 s.

Statistical methods

Differences between groups were evaluated by Mann–Whitney *U*-test. Significance was assumed at values of $p < 0.05$.

Results

Behavioral and morphological changes in the rats infused with KA

Because infusion of 1.5 mM KA did not cause any change in the rat for up to 8 weeks of continuous infusion, and because infusion of 4.5 mM KA induced death as a result of convulsion shortly after operation (data not shown), we adopted the concentration of 3.0 mM KA except in the experiments in which KA was co-infused with CTZ. As compared with the aCSF-infused control rats (aCSF-W/F), which maintained a score of 420 s, the rotarod scores of the KA-infused rats significantly decreased in a time-dependent manner after 2 weeks of KA administration in both the KA-W and the KA-F rat groups, reaching a seventh of the control score after 8 weeks (KA-W: week 0, 420 s, $n = 15$; week 2, 237.3 ± 40.4 s, mean ± SEM, $n = 15$; week 4, 205.4 ± 45.9 s, $n = 10$; week 8, 67.2 ± 19.0 s, $n = 5$) (KA-F: week 0, 420 s, $n = 10$; week 2, 179.7 ± 48.4 s, $n = 10$; week 4, 176.2 ± 40.1 s, $n = 5$) ($p < 0.001$; Fig. 1). Moreover, rats infused with KA developed complete paralysis of the hindlimbs by the end stage, whereas none of the rats showed either sensory deficits or urinary incontinence (data not shown).

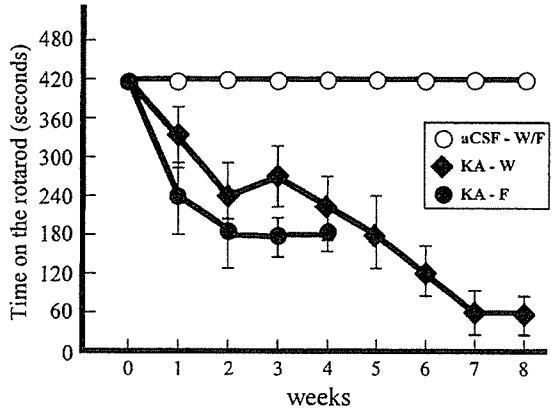

Fig. 1 Time-dependent motor deficit in kainic acid (KA)-infused rats. The rotarod scores of the KA-infused rats were significantly decreased in a time-dependent manner after 2 weeks of KA administration in both the Wistar and Fischer rat groups as compared with respective artificial cerebrospinal fluid (aCSF)-infused control rats ($p < 0.001$). The rotarod speed was 16 rpm.The values plotted on the graph represent the mean rotarod score; error bars indicate the SD. ◆, KA-infused Wistar rats; ●, KA-infused Fischer rats; ○, aCSF-infused Wistar/Fischer rats.

The motor neurons of the KA-F4 and the KA-W8 rats that displayed selective motor dysfunction exhibited morphological changes, including cytoplasmic microvacuolation, loss of Nissl substance and accumulation of glial cells around the degenerating neurons (Figs 2a and c), whereas neurons in the dorsal horn, including small neurons in the substantia gelatinosa of the same rats, appeared morphologically normal (Figs 2a and b). Axons in the fifth lumber ventral root of the KA-W8 rats were severely damaged and displayed a reduction in large myelinated fibers as compared with control rats (Figs 2d and e). Moreover, the number of large motor neurons was significantly reduced in the ventral horn of KA-F4 and KA-W8 rats (KA-F4, 4.8 ± 0.2; aCSF-F4, 6.2 ± 0.2; KA-W8, 3.2 ± 0.1; aCSF-W8, 6.0 ± 0.2; mean ± SEM; $n = 5$) ($p < 0.001$; Fig. 2f) but not in that of either KA-F2 or KA-W4 rats ($p > 0.1$; Fig. 2f). Taken together, these findings show that the KA-infused rats exhibited selective impairment in motor function, which is probably a result of the selective loss of motor neurons in the spinal cord.

Behavioral and morphological changes in the rats co-infused with KA and antagonists

Rats that were infused with KA and NBQX, a potent antagonist for AMPA and KA receptors, showed significantly higher rotarod scores after 3 weeks as compared with those infused with KA alone, whereas those infused with KA and APV, an NMDA receptor antagonist, did not differ from the KA-infused control rats (Fig. 3). By contrast, rats co-infused with CTZ, an AMPA receptor desensitization blocker, and the lower concentration of KA (1.5 mM KA + 1.5 mM CTZ) exhibited very low rotarod scores after 1 week, hence the co-infusion of CTZ and KA seemed to induce a more rapid decline of motor function as compared with the infusion of a higher concentration of KA alone (3 mM KA) (at week 1, $p < 0.05$; Fig. 3). Furthermore, rats that were infused with CTZ alone (1.5 mM CTZ) showed slightly, if any, and only transiently, lower rotarod scores as compared with aCSF-infused control rats (Fig. 3).

The morphometry of large neurons demonstrated that the decrease in the number of motor neurons was significantly less extensive in the KA/NBQX group than in the KA group after 4 weeks (KA, 4.8 ± 0.2; KA/NBQX, 5.6 ± 0.1; mean ± SEM; $n = 5$; $p < 0.001$), but not after 2 weeks (Fig. 4a). Although the concentration of KA in the KA/CTZ group was half of that in the KA-alone group, after 4 weeks the number of motor neurons in the KA/CTZ group tended to be lower than that in the KA group, and was significantly lower than that in the aCSF control and CTZ alone group (Fig. 4a). Moreover, motor neurons in the KA/CTZ group exhibited more severe morphological changes than did motor neurons in the KA-F4 (Fig. 4b) and KA-W8 groups (Fig. 2c), including numerous large cytoplasmic vacuoles with condensation of Nissl substance (Fig. 4c). After 4 weeks, the ventral roots of the KA/CTZ rats displayed marked axonal degeneration with loss of fibers as compared with the control rats (Figs 4d and e), which appeared rather more severe than the changes seen in the KA-W8 group (Fig. 2e).

Neuronal mRNA expression profile of AMPA receptor subunits

In motor neurons of the KA-infused groups (KA-W2, KA-W4, KA-W8, KA-F2 and KA-F4), the quantities of total AMPA receptor subunit mRNA (GluRs) expressed relative to the β-actin baseline were significantly greater than those in the respective aCSF control groups (aCSF-W2, aCSF-W4, aCSF-W8, aCSF-F2 and aCSF-F4) (Fig. 5a). Among the AMPA receptor subunits GluR1, GluR2, GluR3 and GluR4, only the quantity of GluR3 mRNA relative to β-actin was significantly increased in all of the KA-infused groups as compared with their respective aCSF control groups (KA-W vs. aCSF-W: 2 weeks, $39.6 \pm 3.8 \times 10^{-3}$ vs. $25.2 \pm 2.1 \times 10^{-3}$; 4 weeks, $41.8 \pm 4.6 \times 10^{-3}$ vs. $21.5 \pm 1.0 \times 10^{-3}$; 8 weeks, $44.8 \pm 3.8 \times 10^{-3}$ vs. $25.8 \pm 1.8 \times 10^{-3}$; KA-F vs. aCSF-F: 2 weeks, $33.8 \pm 1.2 \times 10^{-3}$ vs. $21.7 \pm 2.0 \times 10^{-3}$; 4 weeks, $46.3 \pm 2.2 \times 10^{-3}$ vs. $26.3 \pm 1.4 \times 10^{-3}$; mean ± SEM; $n = 5$ in each) ($p < 0.001$; Fig. 5a). Because the quantities of GluR1, GluR2 and GluR4 did not change in any of the KA-infused groups, the increase in total AMPA receptor subunit mRNA in these groups was caused by the selective increase in GluR3 mRNA. This molecular change resulted in a significant decrease in the proportion of GluR2

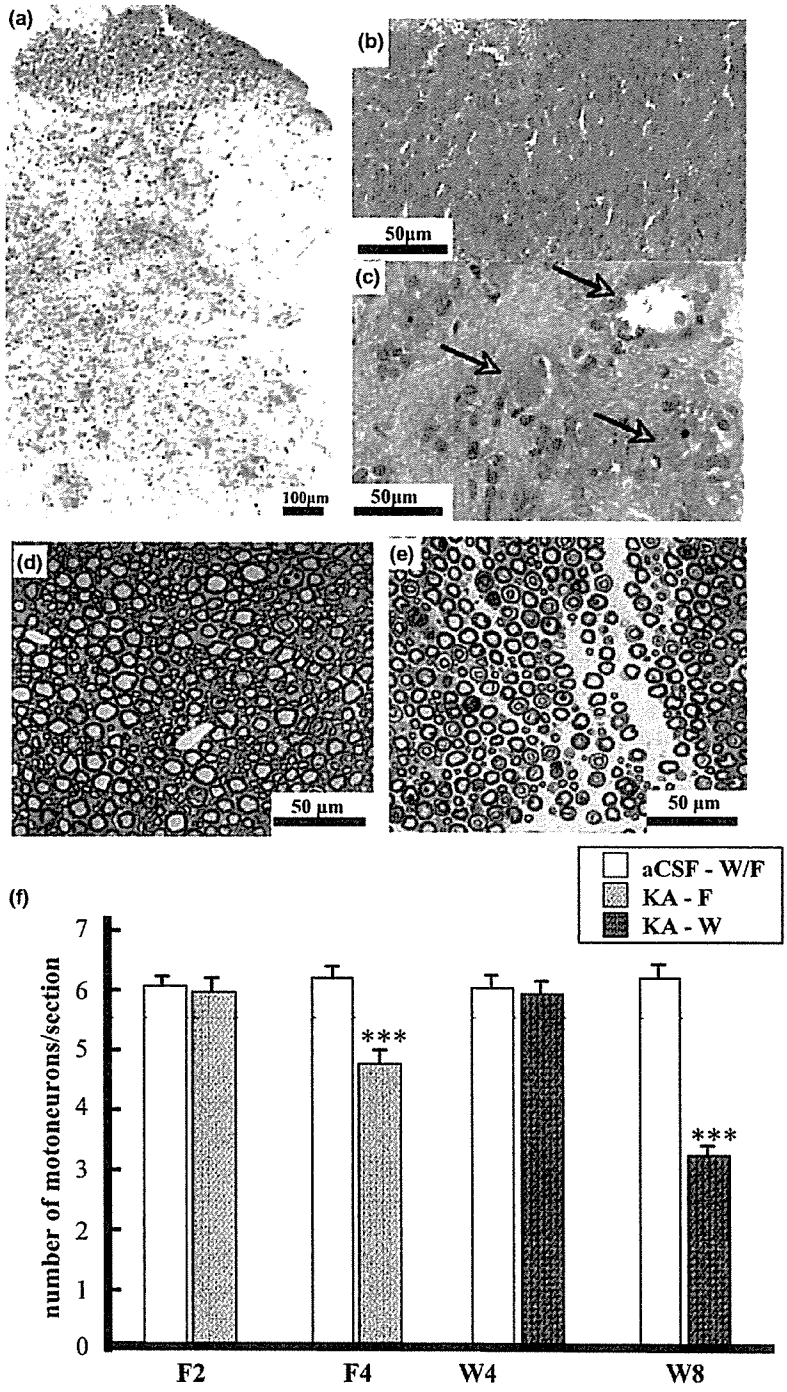

Fig. 2 Morphological changes in the kainic acid (KA)-infused rats. (a–c) Sections stained with hematoxylin and eosin demonstrate that motor neurons in the lumber spinal cords (L5 segment) of a KA-W8 rat exhibited severe morphological changes, including microvacuolation, loss of Nissl substance and glial margination, indicated by the arrows in panel (c), whereas neurons in the dorsal horn appeared intact (a and b). (d and e) Toluidine blue staining of an epon-embedded section of the L5 ventral root of an aCSF-W8 rat (d) and a KA-W8 rat (e) displaying axonal degeneration with a reduction in large myelinated fibers. (f) As compared with aCSF-infused controls, the number of motor neurons was not significantly different in KA-infused Fischer rats at 2 weeks (F2), but was significantly reduced at 4 weeks (F4) (***$p < 0.001$). Similarly, in the Wistar rats, the number of motor neurons was decreased between 4 weeks (W4) and 8 weeks (W8) in the KA-infused rats as compared with aCSF-infused control rats (***$p < 0.001$). The number of neurons with an identifiable nucleolus in a 20-μm-thick section of the L5 segment was expressed in each group. KA-W, KA-infused Wistar rats; KA-F, KA-infused Fischer rats; aCSF-W/F, aCSF-infused Wistar/Fischer rats.

mRNA relative to the total AMPA receptor subunit mRNA in all of the KA-infused groups (Fig. 5b). By contrast, there was no difference in the mRNA expression profile of AMPA receptor subunits including GluR3 mRNA between the KA-infused rats and their controls in either the substantia gelatinosa or the funiculus of the spinal cord (Figs 5c and d).

Discussion

The motor selective behavioral and neuropathological changes induced in this rat model are hallmarks of the clinico-pathological changes seen in ALS. In addition, the delayed and progressive nature of these changes mimics ALS,

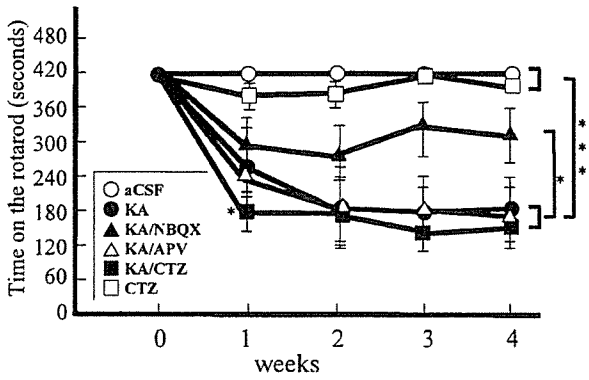

Fig. 3 Motor deficits in Fischer rats after co-infusion of kainic acid (KA) with various compounds. As compared with the KA-alone group, KA/6-nitro-7-sulfamobenso(f)quinoxaline-2,3-dione (NBQX)-infused rats exhibited significantly higher rotarod scores after 3 weeks of administration (*$p < 0.05$), whereas KA/APV-infused rats displayed the same level ($p > 0.1$). The rats co-infused with cyclothiazide (CTZ) and a lower concentration of KA (1.5 mM KA + 1.5 mM CTZ) displayed a more rapid decline in rotarod scores at week 1 as compared with those infused with a higher concentration of KA alone (3 mM KA) (*$p < 0.05$). In addition, infusion of CTZ alone (1.5 mM CTZ) slightly and only transiently decreased the rotarod score as compared with the aCSF-infused control. ●, KA-infused rats; ▲, KA/NBQX-infused rats; △, KA/APV-infused rats; ■, KA/CTZ-infused rats; □, CTZ-infused rats; ○, aCSF-infused rats. The rotarod speed was 16 rpm. Each value plotted indicates the mean rotarod score; error bars indicate the SD. ***$p < 0.001$ KA vs. aCSF and KA/CTZ vs. CTZ.

suggesting that the KA-infused rat is a clinicopathologically appropriate model for ALS. The fact that motor deficit preceded the neuropathological changes by between 2 and 4 weeks may indicate the dysfunction of motor neurons prior to death and the slow death-inducing process. In addition, the results with Wistar and Fischer rats indicate that it takes around 4 weeks to induce the death of motor neurons by this method, and the motor neuron vulnerability is slightly different among the rat strains.

Our co-infusion experiments strongly suggest that the neuronal degeneration observed was mediated by AMPA receptors, in agreement with the results of KA toxicity in cultured rat hippocampal neurons (Ohno *et al.* 1997). The observation that co-infusion of CTZ exacerbated KA toxicity lends further support to a mechanism of AMPA receptor-mediated neurotoxicity. CTZ is a desensitization blocker of AMPA receptors, particularly of the flip splice variants (Partin *et al.* 1994), and does not exhibit neurotoxicity by itself as is observed in cultured neurons (May and Robison 1993; Brorson *et al.* 1995) but enhances KA-induced neurotoxicity with a leftward shift of the KA dose–response curve in cultured neurons (Ohno *et al.* 1998). Because both the flip and flop variants of each AMPA receptor subunit are expressed in rat spinal motor neurons (Tölle *et al.* 1993), CTZ probably exacerbates the neurotoxicity of KA via its desensitization effects on AMPA receptors.

We and other researchers have investigated the neurotoxic effects of various glutamate receptor agonists on spinal neurons *in vivo* and found that glutamate receptor agonists induce the degeneration of different subsets of spinal neurons depending on the route and the duration of administration (Kwak *et al.* 1992; Nakamura *et al.* 1994; Kwak and Nakamura 1995a,b; Hirata *et al.* 1997; Corona and Tapia 2004). Although intrathecal infusion of KA for a brief period induces long-standing damage in spinal motor neurons, it also severely affects interneurons (Kwak and Nakamura 1995b). Because interneurons appeared to be intact after two months of intrathecal KA infusion in the present study, it is likely that in accordance with the results in the cultured neurons (Terro *et al.* 1998), the subtoxic dose of KA that we used here may have selectively activated motor neurons without non-specifically activating interneurons.

An increase in intracellular Ca^{2+} concentration owing to an influx through Ca^{2+}-permeable AMPA receptors has been demonstrated to play a pivotal role in AMPA receptor-mediated neuronal death in cultured motor neurons (Carriedo *et al.* 1996; Van Den Bosch *et al.* 2000). It is likely therefore that long-term administration of KA will induce an increase of Ca^{2+} influx through AMPA receptors, thereby causing the death of motor neurons. Here, we found that the expression of GluR3 mRNA expression was persistently increased in motor neurons, at least from week 2 of KA infusion when no motor neuron death was detected. Up-regulation of GluR3 mRNA was observed only in motor neurons and not in either dorsal horn neurons or in white matter, which morphologically remained intact throughout the experimental period, suggesting that this molecular change is probably caused by the long-term activation of motor neurons by KA. An increase in GluR3 mRNA has been reported in the motor neurons of mice transgenic for mutated human *SOD1* (SOD1G93 A mice) (Spalloni *et al.* 2004), and these motor neurons display an increased vulnerability to excitotoxicity (Spalloni *et al.* 2004). In addition, the survival of these mice can be prolonged by the administration of GluR3 antisense protein nucleic acid (Rembach *et al.* 2004). These findings suggest that an increase in GluR3 mRNA in motor neurons is tightly associated with the mechanism underlying the selective degeneration of motor neurons.

GluR2 plays a critical role both in controlling the assembly and trafficking of AMPA receptors in hippocampal neurons (Sans *et al.* 2003), and in regulating Ca^{2+} permeability (Hollmann *et al.* 1991; Verdoorn *et al.* 1991; Burnashev *et al.* 1992). Furthermore, cultured neurons derived from GluR2-deficient mice are more vulnerable to excitotoxicity than those derived from wild-type animals (Iihara *et al.* 2001; Van Damme *et al.* 2005), and mice deficient for GluR2 RNA editing at the Q/R site die young as a result of premature neuronal death (Brusa *et al.* 1995). Therefore, an

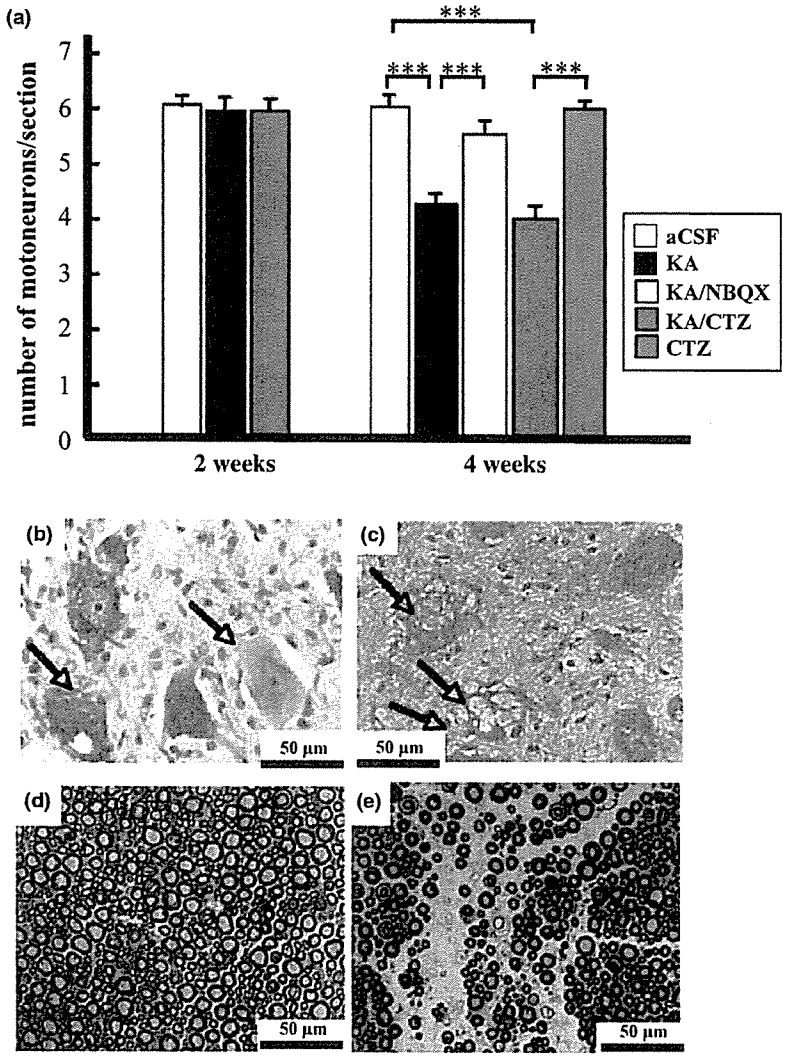

Fig. 4 Effects of α-amino-3-hydroxy-5-methyl-4-isoxazole propionic acid (AMPA) receptor-acting compounds on kainic acid (KA)-induced neurotoxicity in Fischer rats. Co-infusion of 6-nitro-7-sulfamobenso(f)quinoxaline-2,3-dione (NBQX) rescued the neuropathological changes in motor neurons of KA-infused Fischer rats (KA-F), whereas co-infusion of cyclothiazide (CTZ) worsened the changes. (a) The number of motor neurons was not decreased by week 2 in all the groups, whereas it was significantly decreased by week 4 in KA- and KA/CTZ-infused groups. The reduction in the number of motor neurons in KA-F4 was significantly ameliorated by co-infusion of NBQX (***$p < 0.001$). The number of motor neurons in the CTZ alone group was the same as that in the artificial cerebrospinal fluid (aCSF) control, whereas that in the KA/CTZ-infused group was significantly less than in the aCSF control (***$p < 0.001$) but was the same as that in the KA-alone group ($p > 0.1$). KA, KA-infused rats; KA/NBQX, KA/NBQX-infused rats; KA/APV, KA/APV-infused rats; KA/CTZ, KA/CTZ-infused rats; CTZ, CTZ-infused rats; aCSF, aCSF-infused rats. (b and c) Motor neurons in a rat infused with KA (1.5 mM)/CTZ (1.5 mM) for 4 weeks (c) exhibited more severe morphological changes as compared with motor neurons in a rat infused with KA (3 mM) for the same period (b), including marked cytoplasmic vacuolation with condensation of Nissl substance (arrows). (d and e) A ventral root from a KA/CTZ-infused rat at week 4 (e) displayed marked axonal degeneration with loss of fibers as compared with a ventral root from an aCSF-infused control rat at week 4 (d).

increase in GluR3 mRNA may result in a reduction in the relative proportion of GluR2 among AMPA receptor subunits, thereby increasing the proportion of GluR2-lacking, Ca^{2+}-permeable AMPA receptors among the functional AMPA receptors expressed in the motor neurons of KA-infused rats (Fig. 5b). Indeed, the survival of human *SOD1*G93 *A* transgenic mice can be prolonged by the overexpression of GluR2 (Tateno *et al.* 2004), whereas mice that are additionally deficient for GluR2 show decreased survival as compared with those transgenic for human *SOD1*G93 *A* alone (Van Damme *et al.* 2005). Thus, it seems likely that long-term infusion of KA induces the degeneration of motor

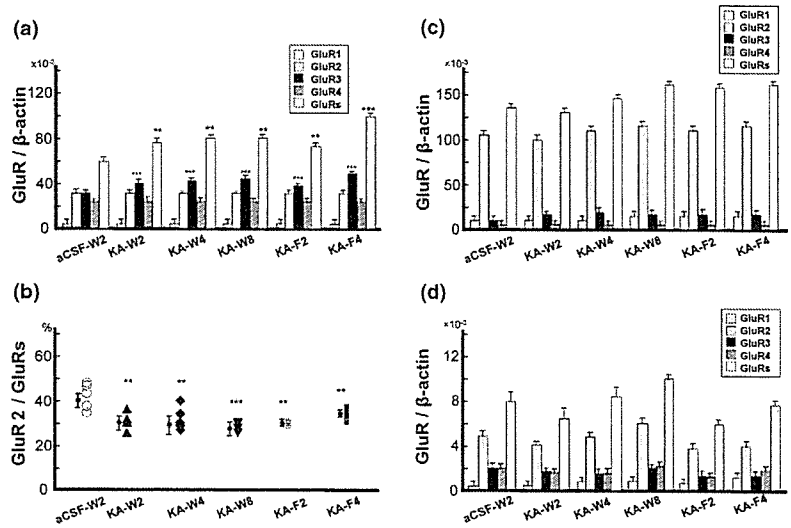

Fig. 5 Quantitative measurement of the expression of α-amino-3-hydroxy-5-methyl-4-isoxazole propionic acid (AMPA) receptor subunit mRNA. (a) In motor neurons of each kainic acid (KA) group, the quantity of total AMPA receptor subunit mRNA and that of GluR3 mRNA relative to the β-actin baseline were significantly greater than those in their artificial cerebrospinal fluid (aCSF) controls (only aCSF-W2 is illustrated for simplicity) (**$p < 0.01$, ***$p < 0.001$). The expression of GluR1, GluR2 or GluR4 in each KA group did not differ from that in the respective aCSF control group. (b) The proportion of GluR2 mRNA relative to the total AMPA receptor subunit mRNA was significantly decreased in the motor neurons of each KA group as compared with their respective aCSF control group (**$p < 0.01$). (c and d) There was no difference in the mRNA expression profile of AMPA receptor subunits between the KA-infused rats and their respective controls in either the substantia gelatinosa (c) or the funiculus of the spinal cord (d).

neurons via an AMPA receptor-mediated mechanism by increasing the proportion of Ca^{2+}-permeable AMPA receptors in motor neurons; however, how KA increases GluR3 mRNA expression, or rather how KA selectively increases this expression in motor neurons while keeping that in dorsal neurons and white matter cells unchanged, remains to be elucidated. Because rat motor neurons express significantly lower quantities of GluR2 mRNA and higher quantities of GluR3 mRNA, as compared with other neuronal subsets (Sun *et al.* 2005), the up-regulation of GluR3 mRNA that presumably reflects an increased level of GluR3 protein may lead to a more marked reduction in the proportion of GluR2, and in turn to a higher proportion of GluR2-lacking, Ca^{2+}-permeable AMPA receptors in motor neurons after KA infusion. The characteristics of motor neurons with a low relative abundance of GluR2 may explain, in part, the selective vulnerability of these cells to AMPA receptor-mediated excitotoxicity.

Another factor influencing the Ca^{2+} permeability of AMPA receptors is the status of GluR2 mRNA editing at the Q/R site. Recently, we have demonstrated that a significant reduction in RNA editing of GluR2 at the Q/R site occurs, in a disease-specific and neuronal class-selective manner, in the motor neurons of patients with sporadic ALS (Kawahara *et al.* 2004, 2006). In addition, the number of neurons was significantly reduced in the ventral horn of the spinal cord of mice transgenic for artificial Ca^{2+}-permeable GluR-B(N) minigenes (Feldmeyer *et al.* 1999; Kuner *et al.* 2005). It is likely that this molecular change is closely relevant to the pathoetiology of ALS; however, we did not find any reduction in GluR2 editing efficiency in the motor neurons of KA-infused rats in this study (data not shown). Therefore, although long-term activation of AMPA receptors *per se* induces the death of motor neurons both *in vitro* and *in vivo*, the underlying mechanism is probably an alteration in the relative proportion of AMPA receptor subunits, and not a reduction in RNA editing. In addition to GluR3 up-regulation (Spalloni *et al.* 2004), a lack of reduction in GluR2 RNA editing (Kawahara *et al.* 2006) suggests the participation of an AMPA receptor-mediated neuronal death mechanism similar to that present in rats with mutated SOD1-associated familial ALS (ALS1). In this respect, the KA-infused rat is a model for ALS1 rather than sporadic ALS. There seems to be different Ca^{2+}-permeable AMPA receptors that mediate neuronal death, including those caused by underedited GluR2 and those caused by a lack of GluR2. It seems likely that the underediting of GluR2 mRNA specifically seen in sporadic ALS motor neurons (Kawahara *et al.* 2004) is not caused by long-term AMPA receptor activation but rather by a defect intrinsic to motor neurons in patients with sporadic ALS.

28

Acknowledgements

We thank Dr Jun Shimizu for valuable discussion. This study was supported, in part, by a grant-in-aid for Scientific Research on Priority Areas from the Ministry of Education, Culture, Sports, Science and Technology of Japan (14017020, 15016030 and 16015228 to SK).

References

Broom W. J., Parton M. J., Vance C. A., Russ C., Andersen P. M., Hansen V., Leigh P. N., Powell J. F., Al-Chalabi A. and Shaw C. E. (2004) No association of the SOD1 locus and disease susceptibility or phenotype in sporadic ALS. *Neurology* **63**, 2419–2422.

Brorson J. R., Manzolillo P. A., Gibbons S. J. and Miller R. J. (1995) AMPA receptor desensitization predicts the selective vulnerability of cerebellar Purkinje cells to excitotoxicity. *J. Neurosci.* **15**, 4515–4524.

Brusa R., Zimmermann F., Koh D., Feldmeyer D., Gass P., Seeburg P. and Sprengel R. (1995) Early-onset epilepsy and postnatal lethality associated with an editing-deficient GluR-B allele in mice. *Science* **270**, 1677–1680.

Burnashev N., Khodorova A., Jonas P., Helm P., Wisden W., Monyer H., Seeburg P. and Sakmann B. (1992) Calcium-permeable AMPA-kainate receptors in fusiform cerebellar glial cells. *Science* **256**, 1566–1570.

Carriedo S. G., Yin H. Z. and Weiss J. H. (1996) Motor neurons are selectively vulnerable to AMPA/kainate receptor-mediated injury in vitro. *J. Neurosci.* **16**, 4069–4079.

Corona J. C. and Tapia R. (2004) AMPA receptor activation, but not the accumulation of endogenous extracellular glutamate, induces paralysis and motor neuron death in rat spinal cord in vivo. *J. Neurochem.* **89**, 988–997.

Feldmeyer D., Kask K., Brusa R., Kornau H. C., Kolhekar R., Rozov A., Burnashev N., Jensen V., Hvalby O., Sprengel R., *et al.* (1999) Neurological dysfunctions in mice expressing different levels of the Q/R site-unedited AMPAR subunit GluR-B. *Nat. Neurosci.* **2**, 57–64.

Gurney M. E., Pu H., Chiu A. Y., Dal Canto M. C., Polchow C. Y., Alexander D. D., Caliendo J., Hentati A., Kwon Y. W., Deng H. X., *et al.* (1994) Motor neuron degeneration in mice that express a human Cu,Zn superoxide dismutase mutation. *Science* **264**, 1772–1775.

Hashida H., Goto J., Suzuki T., Jeong S., Masuda N., Ooie T., Tachiiri Y., Tsuchiya H. and Kanazawa I. (2001) Single cell analysis of CAG repeat in brains of dentatorubral-pallidoluysian atrophy (DRPLA). *J. Neurol. Sci.* **190**, 87–93.

Hirata A., Nakamura R., Kwak S., Nagata N. and Kamakura K. (1997) AMPA receptor-mediated slow neuronal death in the rat spinal cord induced by long-term blockade of glutamate transporters with THA. *Brain Res.* **771**, 37–44.

Hollmann M., Hartley M. and Heinemann S. (1991) Ca2+ permeability of KA-AMPA-gated glutamate receptor channels depends on subunit composition. *Science* **252**, 851–853.

Howland D. S., Liu J., She Y., Goad B., Maragakis N. J., Kim B., Erickson J., Kulik J., DeVito L., Psaltis G., *et al.* (2002) Focal loss of the glutamate transporter EAAT2 in a transgenic rat model of SOD1 mutant-mediated amyotrophic lateral sclerosis (ALS). *Proc. Natl Acad. Sci. USA* **99**, 1604–1609.

Iihara K., Joo D. T., Henderson J., Sattler R., Taverna F. A., Lourensen S., Orser B. A., Roder J. C. and Tymianski M. (2001) The influence of glutamate receptor 2 expression on excitotoxicity in Glur2 null mutant mice. *J. Neurosci.* **21**, 2224–2239.

Jackson M., Al-Chalabi A., Enayat Z. E., Chioza B., Leigh P. N. and Morrison K. E. (1997) Copper/zinc superoxide dismutase 1 and sporadic amyotrophic lateral sclerosis: analysis of 155 cases and identification of a novel insertion mutation. *Ann. Neurol.* **42**, 803–807.

Kawahara Y., Kwak S., Sun H., Ito K., Hashida H., Aizawa H., Jeong S.-Y. and Kanazawa I. (2003) Human spinal motoneurons express low relative abundance of GluR2 mRNA: An implication for excitotoxicity in ALS. *J. Neurochem.* **85**, 680–689.

Kawahara Y., Ito K., Sun H., Aizawa H., Kanazawa I. and Kwak S. (2004) Glutamate receptors: RNA editing and death of motor neurons. *Nature* **427**, 801.

Kawahara Y., Sun H., Ito K., Hideyama T., Aoki M., Sobue G., Tsuji S. and Kwak S. (2006) Underediting of GluR2 mRNA, a neuronal death inducing molecular change in sporadic ALS, does not occur in motor neurons in ALS1 or SBMA. *Neurosci. Res.* **54**, 11–14.

Kuner R., Groom A. J., Bresink I., Kornau H. C., Stefovska V., Muller G., Hartmann B., Tschauner K., Waibel S., Ludolph A. C., *et al.* (2005) Late-onset motoneuron disease caused by a functionally modified AMPA receptor subunit. *Proc. Natl Acad. Sci. USA* **102**, 5826–5831.

Kwak S. and Nakamura R. (1995a) Acute and late neurotoxicity in the rat spinal cord in vivo induced by glutamate receptor agonists. *J. Neurol. Sci.* **129**, 99–103.

Kwak S. and Nakamura R. (1995b) Selective degeneration of inhibitory interneurons in the rat spinal cord induced by intrathecal infusion of acromelic acid. *Brain Res.* **702**, 61–71.

Kwak S., Aizawa H., Ishida M. and Shinozaki H. (1992) Acromelic acid, a novel kainate analogue, induces long-lasting paraparesis with selective degeneration of interneurons in the rat spinal cord. *Exp. Neurol.* **116**, 145–155.

May P. C. and Robison P. M. (1993) Cyclothiazide treatment unmasks AMPA excitotoxicity in rat primary hippocampal cultures. *J. Neurochem.* **60**, 1171–1174.

Nagai M., Aoki M., Miyoshi I., Kato M., Pasinelli P., Kasai N., Brown R. H. Jr and Itoyama Y. (2001) Rats expressing human cytosolic copper-zinc superoxide dismutase transgenes with amyotrophic lateral sclerosis: associated mutations develop motor neuron disease. *J. Neurosci.* **21**, 9246–9254.

Nakamura R., Kamakura K. and Kwak S. (1994) Late-onset selective neuronal damage in the rat spinal cord induced by continuous intrathecal administration of AMPA. *Brain Res.* **654**, 279–285.

Nakamura R., Kamakura K., Hirata A. and Kwak S. (1997) Concentration-dependent changes in motor behavior produced by continuous intrathecal infusion of excitatory amino acids in the rat spinal cord. *Brain Res. Protocol.* **1**, 385–390.

Ohno K., Okada M., Tsutsumi R., Kohara A. and Yamaguchi T. (1997) Kainate excitotoxicity is mediated by AMPA- but not kainate-preferring receptors in embryonic rat hippocampal cultures. *Neurochem. Int.* **31**, 715–722.

Ohno K., Okada M., Tsutsumi R., Matsumoto N. and Yamaguchi T. (1998) Characterization of cyclothiazide-enhanced kainate excitotoxicity in rat hippocampal cultures. *Neurochem. Int.* **32**, 265–271.

Partin K. M., Patneau D. K. and Mayer M. L. (1994) Cyclothiazide differentially modulates desensitization of alpha-amino-3-hydroxy-5-methyl-4-isoxazolepropionic acid receptor splice variants. *Mol. Pharmacol.* **46**, 129–138.

Rembach A., Turner B. J., Bruce S., Cheah I. K., Scott R. L., Lopes E. C., Zagami C. J., Beart P. M., Cheung N. S., Langford S. J., *et al.* (2004) Antisense peptide nucleic acid targeting GluR3 delays disease onset and progression in the SOD1 G93A mouse model of familial ALS. *J. Neurosci. Res.* **77**, 573–582.

Roland L., Mitsumoto H. and De Vivo D. (2005) Hereditary and acquired motor neuron diseases, in *Merritt's Neuology*, 11th edn

(Roland L., ed.), pp. 861–870. Lippincott, Williams & Wilkins, Philadelphia.

Sans N., Vissel B., Petralia R. S., Wang Y. X., Chang K., Royle G. A., Wang C. Y., O'Gorman S., Heinemann S. F. and Wenthold R. J. (2003) Aberrant formation of glutamate receptor complexes in hippocampal neurons of mice lacking the GluR2 AMPA receptor subunit. *J. Neurosci.* **23**, 9367–9373.

Sommer B., Kohler M., Sprengel R. and Seeburg P. H. (1991) RNA editing in brain controls a determinant of ion flow in glutamate-gated channels. *Cell* **67**, 11–19.

Spalloni A., Albo F., Ferrari F., Mercuri N., Bernardi G., Zona C. and Longone P. (2004) Cu/Zn-superoxide dismutase (GLY93 – >ALA) mutation alters AMPA receptor subunit expression and function and potentiates kainate-mediated toxicity in motor neurons in culture. *Neurobiol. Dis* **15**, 340–350.

Sun H., Kawahara Y., Ito K., Kanazawa I. and Kwak S. (2005) Expression profile of AMPA receptor subunit mRNA in single adult rat brain and spinal cord neurons in situ. *Neurosci. Res.* **52**, 228–234.

Tateno M., Sadakata H., Tanaka M., Itohara S., Shin R. M., Miura M., Masuda M., Aosaki T., Urushitani M., Misawa H., *et al.*(2004) Calcium-permeable AMPA receptors promote misfolding of mutant SOD1 protein and development of amyotrophic lateral sclerosis in a transgenic mouse model. *Hum. Mol. Genet.* **13**, 2183–2196.

Terro F., Yardin C., Esclaire F., Ayer-Lelievre C. and Hugon J. (1998) Mild kainate toxicity produces selective motoneuron death with marked activation of CA (2+)-permeable AMPA/kainate receptors. *Brain Res.* **809**, 319–324.

Tölle T. R., Berthele A., Zieglgänsberger W., Seeburg P. H. and Wisden W. (1993) The differential expression of 16 NMDA and non-NMDA receptor subunits in the rat spinal cord and in periaqueductal gray. *J. Neurosci.* **13**, 5009–5028.

Van Damme P., Braeken D., Callewaert G., Robberecht W. and Van Den Bosch L. (2005) GluR2 deficiency accelerates motor neuron degeneration in a mouse model of amyotrophic lateral sclerosis. *J. Neuropathol. Exp. Neurol.* **64**, 605–612.

Van Den Bosch L., Vandenberghe W., Klaassen H., Van Houtte E. and Robberecht W. (2000) Ca (2+)-permeable AMPA receptors and selective vulnerability of motor neurons. *J. Neurol. Sci.* **180**, 29–34.

Verdoorn T., Burnashev N., Monye R. H., Seeburg P. and Sakmann B. (1991) Structural determinants of ion flow through recombinant glutamate receptor channels. *Science* **252**, 1715–1718.

ORIGINAL CONTRIBUTION

A Positron Emission Tomography Study on the Role of Nigral Lesions in Parkinsonism in Patients With Amyotrophic Lateral Sclerosis

Takuto Hideyama, MD; Toshimitsu Momose, MD, PhD; Jun Shimizu, MD, PhD; Shoji Tsuji, MD, PhD; Shin Kwak, MD, PhD

Background: Patients with amyotrophic lateral sclerosis (ALS) sometimes exhibit parkinsonism, but the lesion responsible for parkinsonism has not been extensively studied.

Objective: To test whether nigrostriatal system dysfunction is responsible for parkinsonism in ALS.

Design: From the 182 ALS patients who were admitted to our neurology ward during the past 10 years, we extracted all the patients who satisfied the criteria of both parkinsonism and ALS.

Setting: The University of Tokyo Hospital.

Methods: We conducted [^{18}F]L-dopa and [^{11}C]N-methylspiperone positron emission tomography and technetium Tc 99m hexamethylpropyleneamine oxime single-photon emission computed tomography studies on 5 patients with ALS manifesting overt parkinsonism.

Results: Two male and 3 female patients (average age, 63.2±5.8 years) had ALS for an average of 28.6±21.5 months and had parkinsonism for an average of 15.2±11.4 months. Features of their parkinsonism were characterized by outstanding bradykinesia without resting tremor or dementia. The results of positron emission tomography studies indicated normal nigrostriatal function, but those of single-photon emission computed tomography demonstrated decreased blood flow in the frontotemporal cortices.

Conclusion: It is likely that parkinsonism in ALS is due to cortical lesions rather than nigrostriatal dysfunction and that both symptoms are the clinical manifestation of frontotemporal dementia with motor neuron diseases, including classic ALS.

Arch Neurol. 2006;63:1719-1722

PATIENTS WITH AMYOTROPHIC lateral sclerosis (ALS) or motor neuron disease (MND) rarely exhibit clinically overt parkinsonism.[1] Neuropathological studies of ALS report changes in the extramotor systems, including the substantia nigra, but also note rare findings of Lewy bodies in the affected substantia nigra.[2] Neuroimaging studies have demonstrated a subclinical reduction of striatonigral dopaminergic systems in ALS patients without clinically overt parkinsonism.[3] Therefore, it is possible that nigrostriatal system dysfunction occurs in ALS, but is not responsible for parkinsonism. We conducted [^{18}F]L-dopa and [^{11}C]N-methylspiperone positron emission tomography (PET) scans and technetium Tc 99m hexamethylpropyleneamine oxime single-photon emission computed tomography studies on 5 patients who exhibited both parkinsonism and ALS to further clarify the neurophysical effects of these combined conditions.

Author Affiliations:
Department of Neurology, Graduate School of Medicine (Drs Hideyama, Shimizu, Tsuji, and Kwak), and Department of Radiology (Dr Momose), The University of Tokyo, Tokyo, Japan.

METHODS

PATIENTS

Among the 2485 inpatients in the neurology ward of the University of Tokyo Hospital during the past 10 years (1995-2005), 182 patients were diagnosed with probable or definite ALS according to the revised El Escorial criteria.[4] Ten of these 182 patients exhibited clinically overt parkinsonism, and 5 of these patients were studied with PET.

POSITRON EMISSION TOMOGRAPHY

Studies using [^{18}F]L-dopa and [^{11}C]N-methylspiperone PET were performed with a HEADTOME IV (Shimadzu, Kyoto, Japan). Fourteen transaxial images were obtained, with a 6.5-mm interval parallel to the orbitomeatal line. Final resolution of the reconstructed image was 7.5 mm in the transaxial direction and 9.5 mm in the axial direction at full width half maximum. Transmission scans to correct photon attenuation were carried out at the begin-

Table 1. Patient Characteristics

Patient/ Sex/Age, y	Course of ALS	Initial Symptom	Clinical Symptoms of Motor Neuron Disease			Dementia
			BP	UMN	LMN	
1/F/61	5 y	Upper limb weakness	Yes	Yes	Yes	No
2/F/73	7 mo	Dysarthria	Yes	Yes	Yes	No
3/F/59	2.5 y	Gait disturbance (hesitation)	No	Yes	Yes	No
4/M/59	10 mo	Dysphagia	Yes	Yes	Yes	No
5/M/64	3 y	Dysarthria	Yes	Yes	Yes	No

Abbreviations: ALS, amyotrophic lateral sclerosis; BP, bulbar palsy; LMN, lower motor neuron; UMN, upper motor neuron

Table 2. Parkinsonism Characteristics in Patients

Patient	Bradykinesia	Rigidity	Pulsion	Tremor	Course	Levodopa Dose and Effect of Treatment
1	Yes	Yes	Yes	No	2 y	200 mg/d over 6 mo; slightly effective
2	Yes (hesitation)	Yes	Yes	No	4 mo	400 mg/d over 2 mo; no change
3	Yes (hesitation)	Yes	Yes	No	2.5 y	NA
4	Yes	Yes	Yes	No	6 mo	NA
5	Yes	Yes	Yes	No	1 y	200 mg/d over 6 mo; slightly effective

Abbreviation: NA, not applicable.

ning of each study with germanium 68/gallium 68 external rotating sources. [^{11}C]N-methylspiperone (1110 MBq) was injected intravenously and a static image was obtained over a 10-minute period, starting at 85 minutes after the [^{11}C]N-methylspiperone injection. The [^{18}F]L-dopa study was performed on a different day. One hundred twenty minutes after an intravenous injection of 370 MBq of [^{18}F]L-dopa, a 12-minute static image was taken. As previously described,[5] the tissue radioactivity in each region of interest was corrected by subtracting the nonspecific retention in the cerebellar hemisphere; retention values of the caudate and putamen were expressed as the ratio of radioactivity in each region to that in the cerebellum.

RESULTS

Demographic data of the patients are presented in **Table 1**. The 2 male and 3 female patients were 63.2±5.8 years of age (mean ± SD; range, 59-73 years), with a mean ALS duration of 28.6±21.5 months (range, 7-60 months) and mean parkinsonism duration of 15.2±11.4 months (range, 4-30 months). Three patients initially displayed bulbar palsy, 1 had weakness in the lower extremities, and 1 had a gait disturbance (frozen gait type). Parkinsonism appeared after onset of ALS symptoms in 4 patients and at the same time as ALS symptoms in 1 patient. All patients exhibited predominant upper and lower motor neuron signs, and 4 patients had additional bulbar symptoms. Lower motor neuron involvement was demonstrated by needle electromyogram in all patients. Parkinsonism was characterized by severe bradykinesia and moderate muscle rigidity without resting tremor. Four patients had severe disturbance in postural reflex with marked pulsion, 2 patients had outstanding frozen gait, and all 5 patients had moderate muscle rigidity; however, none of the patients had resting tremors. Three patients were treated with levodopa for 2 to 6 months without any significant beneficial effect on their parkinsonism (**Table 2**). None of the patients exhibited overt dementia, and all of them scored within normal ranges in the Mini-Mental State Examination and the Wechsler Adult Intelligence Scales–Revised. All patients exhibited normal brain magnetic resonance images. Both [^{18}F]L-dopa uptake and [^{11}C]N-methylspiperone binding were normal in all areas, including the caudal putamen (**Table 3** and **Figure**). Single-photon emission computed tomography demonstrated a decrease in the cortical blood flow in 4 of 5 patients (Table 3).

COMMENT

Our PET studies indicate that both preganglionic and postganglionic striatonigral dopaminergic systems were preserved in the patients who exhibited overt parkinsonism, in marked contrast to previous studies reporting that [^{18}F]L-dopa uptake was reduced in ALS patients without overt parkinsonism.[3] Clinical and neuropathological studies have presented findings from patients with parkinsonism associated with ALS, including, other than classic type, ALS with dementia, multisystem atrophy, postencephalitic ALS, diffuse Lewy body disease, and familial ALS.[2] Our ALS patients' clinical parkinsonism features were similar to those in the published literature but were atypical when compared with the typical features of Parkinson disease; all of these patients exhibited predominant akinesia, but none of them had exhibited resting tremor or considerable improvement after levodopa treatment. The relatively late age at onset and lack of dementia or autonomic dysfunction were common clinical features. There was a mild to moderate reduction in

Table 3. Positron Emission Tomography (PET) and Single-Photon Emission Computed Tomography (SPECT) Findings of 5 Patients

		[^{18}F]L-dopa		NMSP		SPECT	
Patient	PET Striatum	Left	Right	Left	Right	Cortex	Basal Ganglia
1	Ventral	2.13	2.15	3.73	3.85	Blood flow decreased in areas 4, 6, 8, 10, and in the right cerebellar hemisphere.	Blood flow decreased in the bilateral corpus striatum.
	Intermediate	2.18	2.10	3.78	3.94		
	Dorsal	2.00	1.94	3.40	3.37		
2	Ventral	3.03	3.20	4.09	4.53	Blood flow decreased in the frontal lobe (greater decrease in the right frontal lobe) and in the left cerebellar hemisphere.	Blood flow decreased in the right corpus striatum and in the right thalamus.
	Intermediate	3.20	3.00	4.46	4.70		
	Dorsal	2.96	2.58	3.90	4.09		
3	Ventral	2.49	2.69	4.23	4.25	Blood flow decreased in the bilateral frontal lobe (especially area 6) and in the bilateral temporoparietal lobe.	Normal
	Intermediate	2.62	2.69	4.23	4.25		
	Dorsal	2.40	2.39	3.70	3.86		
4	Ventral	2.15	2.23	4.31	4.18	Normal	Blood flow decreased in the left basal ganglia.
	Intermediate	2.46	2.40	4.44	4.60		
	Dorsal	2.24	2.31	3.79	4.12		
5	Ventral	2.85	2.90	3.23	3.31	Blood flow decreased in the right temporal occipital parietal lobe.	Blood flow decreased in the left basal ganglia.
	Intermediate	3.05	3.10	3.82	3.56		
	Dorsal	2.41	2.56	3.18	3.16		

Abbreviation: NMSP, [^{11}C]N-methylspiperone.

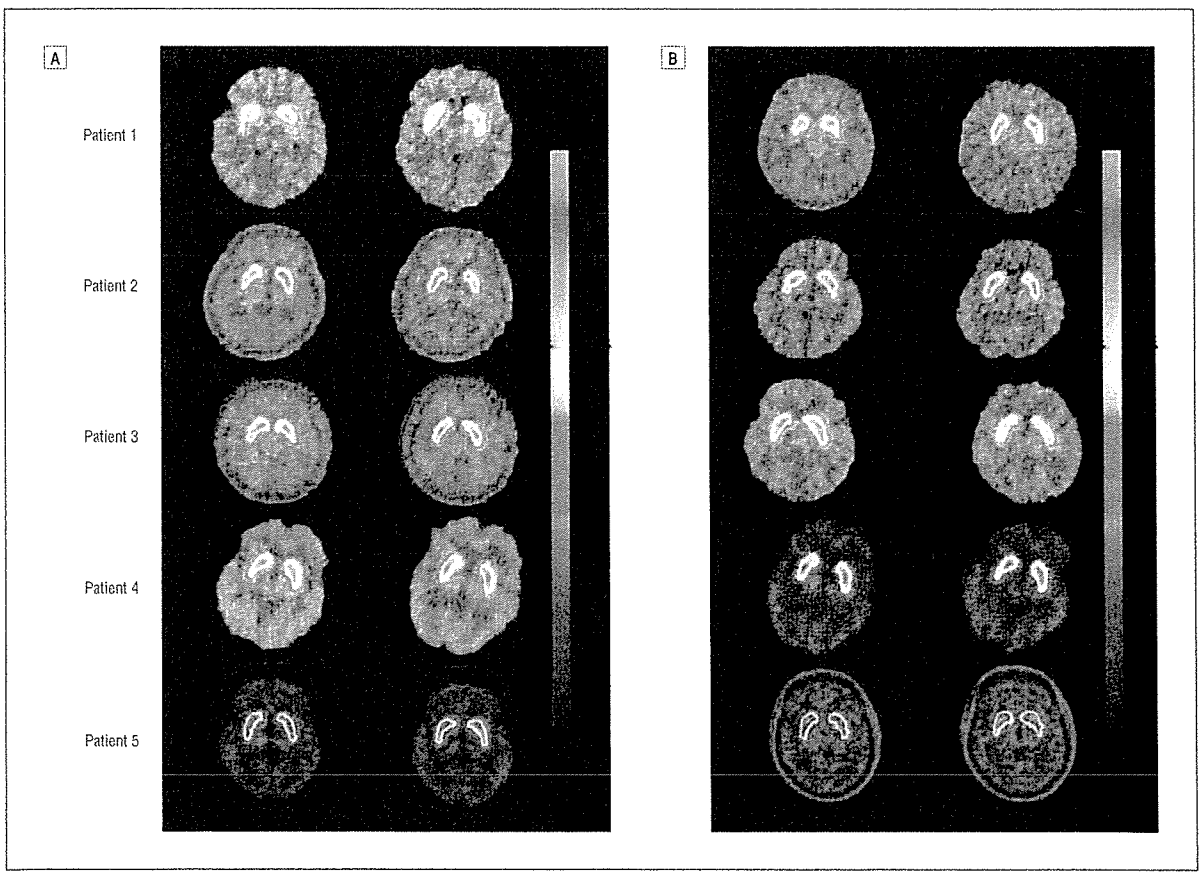

Figure. Positron emission tomography images of study patients. A, [^{18}F]L-dopa images. B, [^{11}C]N-methylspiperone images. Two adjacent sections including the basal ganglia are shown.

the number of neurons in the substantia nigra; Lewy bodies were rarely reported.[2,6] These lines of evidence suggest that parkinsonism in ALS is not likely an association of Parkinson disease with ALS, but is likely due to pathological changes in areas other than the substantia nigra.

In this context, it is worth noting that isolated lesions in the supplementary motor area are associated with clinical features very similar to parkinsonism, dominated by severe akinesia and mild rigidity without resting tremor.[7] Regional cerebral blood flow has been reported to be decreased in the frontal cortices, including the supplementary motor area of patients with Parkinson disease; however, flow could be reversed with antiparkinsonian treatment.[8] Thus, clinical manifestations quite similar to parkinsonism can be produced by isolated cortical lesions in the supplementary motor area. Reduction of regional cerebral blood flow in the frontal and/or temporal cortices extending beyond the primary motor area has been demonstrated in both ALS with dementia and classic ALS without dementia.[9] This observation is in accordance with our single-photon emission computed tomography scan results showing 4 patients with a decrease of regional cerebral blood flow in the frontal and/or temporal cortices.

The degree of regional cerebral blood flow reduction in the frontal and anterior temporal lobes has been reported to correlate with severity of dementia in ALS patients with associated dementia; these blood flow characteristics are indistinguishable from those seen in patients with frontotemporal dementia.[10] Indeed, ALS is not infrequently (approximately 15% of cases) associated with frontotemporal dementia, and involvement of lower motor neurons was found in a group of patients with frontotemporal dementia without a prior diagnosis of ALS.[11] A subclass of frontotemporal dementia with tau-negative and ubiquitin-positive inclusions has been classified as frontotemporal lobar degeneration with motor neuron disease (FTLD-MND) and frontotemporal lobar degeneration with motor neuron disease type (FTLD-MND type), respectively, depending on the presence or absence of clinically overt motor neuron signs.[12] These diagnostic subclasses (FTLD-MND and FTLD-MND type) have been reported to comprise 40% of pathologically proven frontotemporal dementia cases. In addition, patients with frontotemporal dementia frequently exhibit parkinsonism, but neuropathological changes in the substantia nigra were more marked in patients with concomitant dementia irrespective of the presence or absence of parkinsonism, as compared with patients without dementia[13]; hence, reduction of nigrostriatal dopaminergic function may not be associated with parkinsonism. Common pathological changes have been demonstrated in FTLD-MND, FTLD-MND type, and classic ALS without dementia, implying that these diseases comprise a clinicopathological spectrum rather than individual entities.[13]

Taken together, parkinsonism associated with ALS or FTLD-MND may not be due to a dysfunction of the nigrostriatal dopaminergic neurons but rather frontal lesions including the supplementary motor area.

Accepted for Publication: May 30, 2006.
Correspondence: Takuto Hideyama, MD, 7-3-1 Hongo, Bunkyo-Ku, Tokyo 113-8655, Japan (hideyama-int@h.u-tokyo.ac.jp).
Author Contributions: *Study concept and design:* Hideyama and Kwak. *Acquisition of data:* Hideyama, Momose, Shimizu, Tsuji, and Kwak. *Analysis and interpretation of data:* Hideyama, Momose, Shimizu, Tsuji, and Kwak. *Drafting of the manuscript:* Hideyama, Momose, Shimizu, Tsuji, and Kwak. *Critical revision of the manuscript for important intellectual content:* Hideyama, Momose, Shimizu, Tsuji, and Kwak. *Statistical analysis:* Hideyama. *Obtained funding:* Kwak. *Administrative, technical, and material support:* Hideyama, Momose, Shimizu, Tsuji, and Kwak. *Study supervision:* Momose, Shimizu, Tsuji, and Kwak.
Financial Disclosure: None reported.
Acknowledgment: We are grateful to Dr Shigeo Murayama for valuable discussion and for the efforts of the young neurologists in our department.

REFERENCES

1. Eisen A, Calne D. Amyotrophic lateral sclerosis. Parkinson's disease and Alzheimer's disease: phylogenetic disorders of the human neocortex sharing many characteristics. *Can J Neurol Sci.* 1992;19(1 Suppl):117-123.
2. Williams TL, Shaw PJ, Lowe J, Bates D, Ince PG. Parkinsonism in motor neuron disease: case report and literature review. *Acta Neuropathol (Berl).* 1995;89:275-283.
3. Takahashi H, Snow BJ, Bhatt MH, Peppard R, Eisen A, Calne DB. Evidence for a dopaminergic deficit in sporadic amyotrophic lateral sclerosis on positron emission scanning. *Lancet.* 1993;342:1016-1018.
4. Brooks BR. Versailles minimal dataset for diagnosis of ALS: a distillate of the 2nd Consensus Conference on accelerating the diagnosis of ALS, Versailles 2nd Consensus Conference participants. *Amyotroph Lateral Scler Other Motor Neuron Disord.* March 2000;(suppl 1):S79-S81.
5. Yoshimura M, Yamamoto T, Iso-o N, et al. Hemiparkinsonism associated with a mesencephalic tumor. *J Neurol Sci.* 2002;197:89-92.
6. Yoshida M. Amyotrophic lateral sclerosis with dementia: the clinicopathological spectrum. *Neuropathology.* 2004;24:87-102.
7. Dick JP, Benecke R, Rothwell JC, Day BL, Marsden CD. Simple and complex movements in a patient with infarction of the right supplementary motor area. *Mov Disord.* 1986;1:255-266.
8. Jenkins IH, Fernandez W, Playford ED, et al. Impaired activation of the supplementary motor area in Parkinson's disease is reversed when akinesia is treated with apomorphine. *Ann Neurol.* 1992;32:749-757.
9. Abrahams S, Goldstein LH, Kew JJ, et al. Frontal lobe dysfunction in amyotrophic lateral sclerosis: a PET study. *Brain.* 1996;119:2105-2120.
10. Vercelletto M, Ronin M, Huvet M, Magne C, Feve JR. Frontal type dementia preceding amyotrophic lateral sclerosis: a neuropsychological and SPECT study of five clinical cases. *Eur J Neurol.* 1999;6:295-299.
11. Lomen-Hoerth C, Anderson T, Miller B. The overlap of amyotrophic lateral sclerosis and frontotemporal dementia. *Neurology.* 2002;59:1077-1079.
12. McKhann GM, Albert MS, Grossman M, Miller B, Dickson D, Trojanowski JQ. Clinical and pathological diagnosis of frontotemporal dementia: report of the Work Group on Frontotemporal Dementia and Pick's Disease. *Arch Neurol.* 2001;58:1803-1809.
13. Mackenzie IR, Feldman H. The relationship between extramotor ubiquitin-immunoreactive neuronal inclusions and dementia in motor neuron disease. *Acta Neuropathol (Berl).* 2003;105:98-102.

ELSEVIER

Calcium-permeable AMPA channels in neurodegenerative disease and ischemia

Shin Kwak[1] and John H Weiss[2]

Compelling evidence supports contributions of glutamate receptor overactivation ('excitotoxicity') to neurodegeneration in both acute conditions, such as stroke, and chronic neurodegenerative conditions, such as amyotrophic lateral sclerosis. However, anti-excitotoxic therapeutic trials, which have generally targeted highly Ca^{2+} permeable NMDA-type glutamate channels, have to date failed to demonstrate impressive efficacy. Whereas most AMPA type glutamate channels are Ca^{2+} impermeable, an evolving body of evidence supports the contention that relatively unusual Ca^{2+} permeable AMPA channels might be crucial contributors to injury in these conditions. These channels are preferentially expressed in discrete neuronal subpopulations, and their numbers appear to be upregulated in amyotrophic lateral sclerosis and stroke. In addition, unlike NMDA channels, Ca^{2+} permeable AMPA channels are not blocked by Mg^{2+}, but are highly permeable to another potentially harmful endogenous cation, Zn^{2+}. The targeting of these channels might provide efficacious new avenues in the therapy of certain neurological diseases.

Addresses
[1] Department of Neurology, Graduate School of Medicine, University of Tokyo, 7-3-1 Hongo, Bunkyo-ku, 113-8655 Tokyo, Japan
[2] 2101 Gillespie Building, University of California, Irvine, CA 92697-4292, USA

Corresponding author: Weiss, John H (jweiss@uci.edu)

Current Opinion in Neurobiology 2006, **16**:281–287

This review comes from a themed issue on
Signalling mechanisms
Edited by Erin M Schuman and Peter H Seeburg

Available online 15th May 2006

0959-4388/$ – see front matter

DOI 10.1016/j.conb.2006.05.004

Introduction

Excessive extracellular exposure to glutamate, an excitatory neurotransmitter, is harmful to neurons and contributes to neurodegeneration in certain diseases of the central nervous system. In amyotrophic lateral sclerosis (ALS), toxic elevations of glutamate appear to result from loss or dysfunction of astrocytic glutamate transporters. In ischemia, rapid glutamate release combined with deficiency in (or even reversal of) uptake causes extracellular glutamate accumulation.

Glutamate activates a number of types of postsynaptic ion channels. Most prominent among these are NMDA (N-methyl-D-aspartic acid)-type glutamate channels, which are highly Ca^{2+} permeable, and AMPA (1-amino-3-hydroxy-5-methyl-4-isoxazole propionic acid)-type glutamate channels, which mediate most rapid excitatory neurotransmission and are generally Ca^{2+} impermeable. However, some AMPA channels are Ca^{2+} permeable and emerging evidence supports the idea that these unusual channels, which are preferentially expressed on discrete populations of neurons, might be crucial contributors to injury in both ALS and ischemia.

It is also apparent that the number of Ca^{2+} permeable AMPA channels is subject to regulation both in response to physiological patterns of synaptic activity and in certain pathological states. Specifically, whereas relatively few Ca^{2+} permeable AMPA channels are normally present on hippocampal pyramidal neurons (HPNs), the number of these channels can increase sharply after ischemia. By contrast, the motor neurons (MNs), which selectively degenerate in ALS, normally do possess substantial numbers of Ca^{2+} permeable AMPA channels. However, recent evidence suggests that the number of these channels might further increase in ALS. In this review, we discuss recent evidence for roles of Ca^{2+} permeable AMPA channels in disease, with particular emphasis on intriguing clues to their roles in ALS and ischemia.

What are Ca^{2+}-permeable AMPA channels, and how are they regulated?

Functional AMPA receptors are homo- or hetero-oligomeric assemblies that are composed of various combinations of four possible subunits, GluR1, GluR2, GluR3 and GluR4. The Ca^{2+} conductance of AMPA receptors differs markedly according to whether the GluR2 subunit is present or not. AMPA receptors that contain at least one GluR2 subunit have low Ca^{2+} conductance, whereas those lacking a GluR2 subunit are Ca^{2+} permeable [1]. These properties of GluR2 are generated post-transcriptionally by RNA editing at the Q/R site in the putative second membrane domain (M2), during which a glutamine (Q) codon is replaced by an arginine (R) codon [1]. The presence of this positively charged residue, the arginine, in the pore of the channel impedes Ca^{2+} permeation (Figure 1). Analyses of the RNA from adult rat, mouse, and human brains have demonstrated that almost all GluR2 mRNA in neurons is edited, whereas in the GluR1, GluR3 and GluR4 subunits glutamine remains at this crucial position. AMPA receptors containing an unedited GluR2 (GluR2Q) have high Ca^{2+} permeability [1,2].

35

Glossary
Permeability transition pore: A large conductance channel through the mitochondrial membranes, persistent opening of which has been associated with mitochondrial disruption, release of the apoptotic mediator, cytochrome C, and cell death.
Ventral root avulsion: An injury causing disruption of the connection among spinal motor neurons, which send their axons out of the spinal cord through the ventral root, and the muscles that they innervate.

Under normal circumstances, most neurons have few Ca^{2+} permeable AMPA channels, reflecting the presence of edited GluR2 subunits and, therefore, arginine impeding Ca^{2+} entry in most of their AMPA channels. Furthermore, AMPA channels are not static, but undergo dynamic regulation through many mechanisms. Levels of Ca^{2+} permeable AMPA channels can be regulated by alterations in receptor trafficking, and a decrease in the number of these channels can occur in response to physiological activation [3], through mechanisms that appear to be dependent upon specific protein–protein interactions with GluR2 [4•,5•]. Indicating the importance of such regulation, insertion of AMPA channels into the synaptic membrane is sensitive to the editing state of the GluR2 Q/R site [6,7]. In contrast to the studies in which physiological activation results in a decrease in the number of postsynaptic Ca^{2+} permeable AMPA channels, recent studies have found that the presence of tumor necrosis factor-alpha (TNF-alpha), a cytokine, can result in membrane insertion of Ca^{2+} permeable AMPA channels in some neurons. This mechanism might promote neuronal injury in pathological conditions associated with elevations of this cytokine [8,9•,10•]. As discussed below, the number of Ca^{2+} permeable AMPA channels can also be regulated at the level of GluR2 mRNA expression, as is hypothesized to be the case in ischemia [11,12], or by defects in mRNA editing, as is hypothesized to be the case in ALS [13••,14•,15].

How might Ca^{2+} permeable AMPA channel activation injure neurons?

Although mechanisms of excitotoxic neuronal injury are complex and not completely understood, intracellular Ca^{2+} overload is an important trigger. With substantial intracellular Ca^{2+} loading, Ca^{2+} is taken up into mitochondria, and can cause generation of reactive oxygen species (ROS) or opening of the permeability transition pore (see glossary) and release of apoptotic mediators such as cytochrome C. With more modest intracellular Ca^{2+} accumulation, injury could be mediated by other mechanisms, including generation of nitric oxide (NO), with consequent activation of poly(ADP-ribose) polymerase (PARP) and release of mitochondrial apoptosis inducing factor (AIF) [16].

Another way in which Ca^{2+} permeable AMPA channels might mediate injury is by serving as entry routes for the divalent cation, Zn^{2+}, which is co-released with glutamate at certain excitatory synapses. Zn^{2+} accumulates in HPNs in ischemia and epilepsy, both conditions in which Zn^{2+} chelators are neuroprotective [17,18]. Whereas the Zn^{2+} accumulation is probably due to a combination of 'translocation' across the synapse and mobilization from

Figure 1

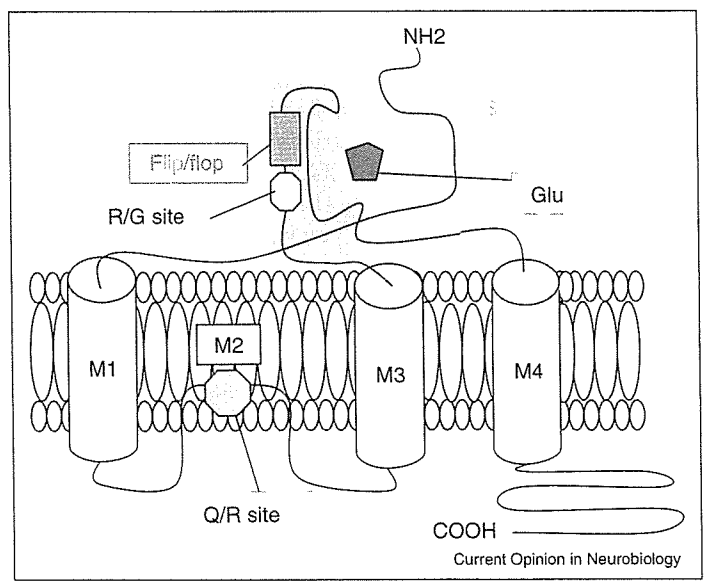

Structure of an AMPA receptor subunit (GluR2). The Q/R site is localized in the P-loop or putative second membrane domain (M2), which faces the channel pore of the AMPA receptor. Permeation of divalent cations is prevented when positively charged arginine (R) is placed in the Q/R site (through editing of the GluR2 mRNA), but can permeate when neutral glutamine (Q) is present. Reprinted with permission from Figure 1b in Nishimoto *et al.* [50].

intracellular pools [18], Ca^{2+} permeable AMPA channels are highly Zn^{2+} permeable, and might thus be the primary route for entry of synaptic Zn^{2+} [19–21]. Similar to Ca^{2+}, Zn^{2+} appears to induce injury through a number of mechanisms, including enzyme induction, ROS generation and PARP activation [22]. Intriguingly, however, in comparison to Ca^{2+}, Zn^{2+} is far more potent at inducing disruption of mitochondrial function, raising the possibility that mitochondrial effects contribute prominently to the degeneration resulting from strong intracellular Zn^{2+} accumulation [20,23–25].

There are several reasons that Ca^{2+} permeable AMPA channels might be expected to play greater roles in neurodegeneration than NMDA channels. First, an increase in their number, as appears to happen in sporadic ALS and ischemia, would subject neurons to new metabolic burdens, possibly tipping the balance towards degeneration. Second, because NMDA channels are subject to voltage-dependent block by Mg^{2+} ions, they permit little Ca^{2+} entry in the absence of strong postsynaptic depolarization. Finally, the high Zn^{2+} permeability of Ca^{2+} permeable AMPA channels does not apply to NMDA channels, which are blocked by Zn^{2+}.

Role in amyotrophic lateral sclerosis

An excitotoxic model of ALS was supported by the observation that astrocytic glutamate uptake is deficient in the motor cortices and spinals cords of ALS patients [26]. Furthermore, the finding that MNs are selectively vulnerable to injury caused by AMPA/kainate receptor activation [27,28] suggested a crucial role for these receptors. This vulnerability is possibly caused by the fact that MNs possess substantial numbers of Ca^{2+} permeable AMPA channels [27,29,30], a finding consistent with the observation that MNs possess a lower relative abundance of GluR2 mRNA as compared with that in other neuronal subclasses both in humans [31] and in rats [32].

If Ca^{2+} permeable AMPA channels play a crucial role in excitotoxic MN injury, an increase in their number might initiate or accelerate the disease. Recent studies using real-time reverse transcriptase-polymerase chain reaction (RT-PCR) to compare GluR2 mRNA expression between ALS patients and controls found no differences in total GluR2 mRNA levels or the ratio of GluR2 mRNA to total AMPA receptor subunit mRNA [31]. However, these studies did find evidence for a reduction of GluR2 editing efficiency [13••,14•,15], which appeared to be selective for MNs [13••]. Furthermore, the editing defect appeared to be specific to ALS among several neurodegenerative diseases [14•], and to be specific to sporadic disease, as GluR2 mRNA was fully edited in G93A and H46R SOD1 transgenic rat models of familial ALS, and in humans with spinal and bulbar muscular atrophy (SBMA) [33•] (Figure 2).

Figure 2

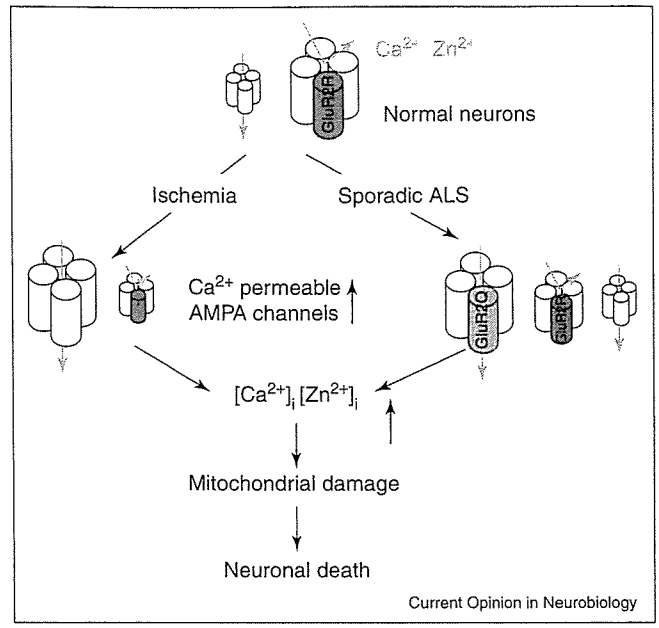

Ca^{2+} or Zn^{2+} influx through AMPA receptors is regulated by the GluR2 subunit. AMPA receptors with GluR2 that has been edited at the Q/R site are Ca^{2+}-impermeable, but those lacking GluR2 entirely or with unedited GluR2 are Ca^{2+}-permeable. Under basal conditions, hippocampal pyramidal neurons (HPNs) have relatively few Ca^{2+} permeable AMPA channels comprising AMPA receptors lacking GluR2, whereas motor neurons (MNs) possess a substantial number of these channels. After ischemia, a decrease in GluR2 mRNA expression in CA1 hippocampal pyramidal neurons results in increased numbers of Ca^{2+} permeable AMPA channels lacking GluR2, contributing to their delayed degeneration (Of note, a recent study suggests that loss of editing efficiency might also contribute to increased Ca^{2+} permeable AMPA channel expression after ischemia; see update). By contrast, MNs in sporadic ALS express considerable unedited GluR2 mRNA, probably resulting in an increased number of Ca^{2+} permeable AMPA channels containing unedited GluR2. In either case, an increase in the proportion of Ca^{2+} permeable AMPA channels enables increased Ca^{2+} and/or Zn^{2+} entry into the cytoplasm, which contributes to neuronal death partly through effects on mitochondria. Red, orange and white cylinders represent edited GluR2, unedited GluR2 and AMPA receptor subunits other than GluR2 (GluR1, 3 or 4), respectively.

Many recent studies support the theory that Ca^{2+} permeable AMPA channels have a crucial role in MN degeneration in diverse conditions. A recent study found ventral root avulsion (see glossary) to cause selective decreases in the GluR2 protein [34], probably contributing to the MN injury in that condition. A Ca^{2+} permeable AMPA channel blocker was found to be protective in a model of virus-induced MN degeneration [35•]. Transgenic animal studies have recently solidified the link between Ca^{2+} permeable AMPA channels and MN loss in SOD1-linked familial forms of ALS. Specifically, mice with modified GluR2 (GluR2-N), which results in production of AMPA channels with enhanced Ca^{2+} permeability, had late life MN degeneration [36••], and crossing either these mice or mice lacking GluR2 entirely with mice with the G93A

Figure 3

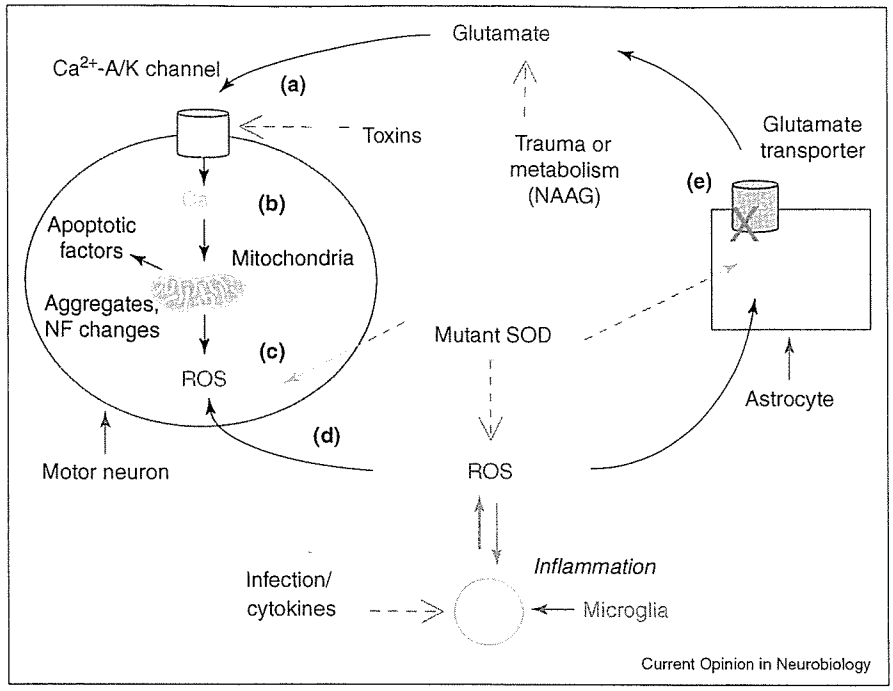

A feed-forward model of ALS pathogenesis. Present observations provide the basis for a feed-forward cycle leading to selective MN injury in ALS. **(a)** Elevations of extracellular glutamate induce **(b)** excessive Ca^{2+} entry into MNs (through Ca^{2+} permeable AMPA channels), where it is taken up by mitochondria, **(c)** with consequent ROS generation and, possibly, activation of apoptotic pathways, either of which would injure the neuron. **(d)** The ROS could pass across the MN plasma membrane and **(e)** disrupt astrocytic glutamate transporters, thereby causing further rises in extracellular glutamate. Such a cycle could, in principle, be triggered at different sites (e.g., via glutamate rises or oxidative stress), and thus might be compatible with a multiplicity of inciting mechanisms (suggested in dashed boxes) leading into a common self propagating disease pathway. Reprinted from [42•] with permission from Elsevier.

SOD1 model of ALS resulted in marked acceleration of the disease [37•]. Conversely, when mice with a decreased number of Ca^{2+} permeable AMPA channels in their MNs (via targeted GluR2 overexpression) were crossed with the G93A mice, the disease was significantly delayed [38•].

Mechanisms through which the presence of Ca^{2+} permeable AMPA channels contributes to excitotoxic MN injury are being elucidated. Although these channels enable rapid Ca^{2+} entry, MNs buffer cytosolic Ca^{2+} loads poorly [39], and consequently much of the Ca^{2+} is readily taken up into mitochondria, resulting in strong ROS generation [40,41]. Furthermore, *in vitro* studies indicated that ROS produced in MNs in response to Ca^{2+} permeable AMPA channel activation might induce oxidative dysfunction of glutamate transporters in surrounding astrocytes [42•]. This mechanism could play a role in the glutamate transport disruption seen in ALS, and provides the basis for a feed-forward cycle that could be integral to progression of the disease [42•] (Figure 3).

Role in ischemia

After transient global ischemia, HPNs, particularly in the CA1 subzone of the hippocampus, conspicuously degenerate, often with a delay of several days. Under basal conditions, HPNs have few Ca^{2+} permeable AMPA channels. However, recent studies suggest that limited numbers of these channels are present, and they appear to be mainly localized to dendritic branches remote from the soma, where they are difficult to detect electrophysiologically [43–45].

Observations that GluR2 mRNA is markedly and selectively downregulated in CA1 HPNs after ischemia have led to an hypothesis that consequent increases in the number of Ca^{2+} permeable AMPA channels contribute to the delayed neurodegeneration [12] (Figure 2). Studies in recent years have provided considerable support to this hypothesis. First, GluR2 protein levels are decreased and AMPA-mediated Ca^{2+} currents are increased after ischemia [11]. Also, increasing the number of Ca^{2+} permeable AMPA channels in CA1 resulted in an increased vulnerability of HPNs to ischemic injury [46], whereas elevating GluR2 levels appeared to be protective [47•]. Finally, some neuroprotection was observed upon addition of a Ca^{2+} permeable AMPA channel blocker many hours to days after the induction of ischemia [48••]. This suggests that new treatments targeting these channels could